

Space Weather and The PROGRESS project idea and concept

ssg.group.shef.ac.uk/progress/html

This project has received funding from the *European Union's Horizon 2020 research and innovation programme* under grant agreement No 637302.

Space Weather

“Just as weather can be expressed as a set of atmospheric parameters that are important not only for our comfort but also determine conditions for the operation of technological systems on the ground and in the atmosphere, **space weather** is expressed by the set parameters relating to the near Earth environment that determine important conditions for many modern technological systems operating on the terrestrial surface (e.g. power grids), in the atmosphere (aviation) and in the space (satellites, manned missions).”

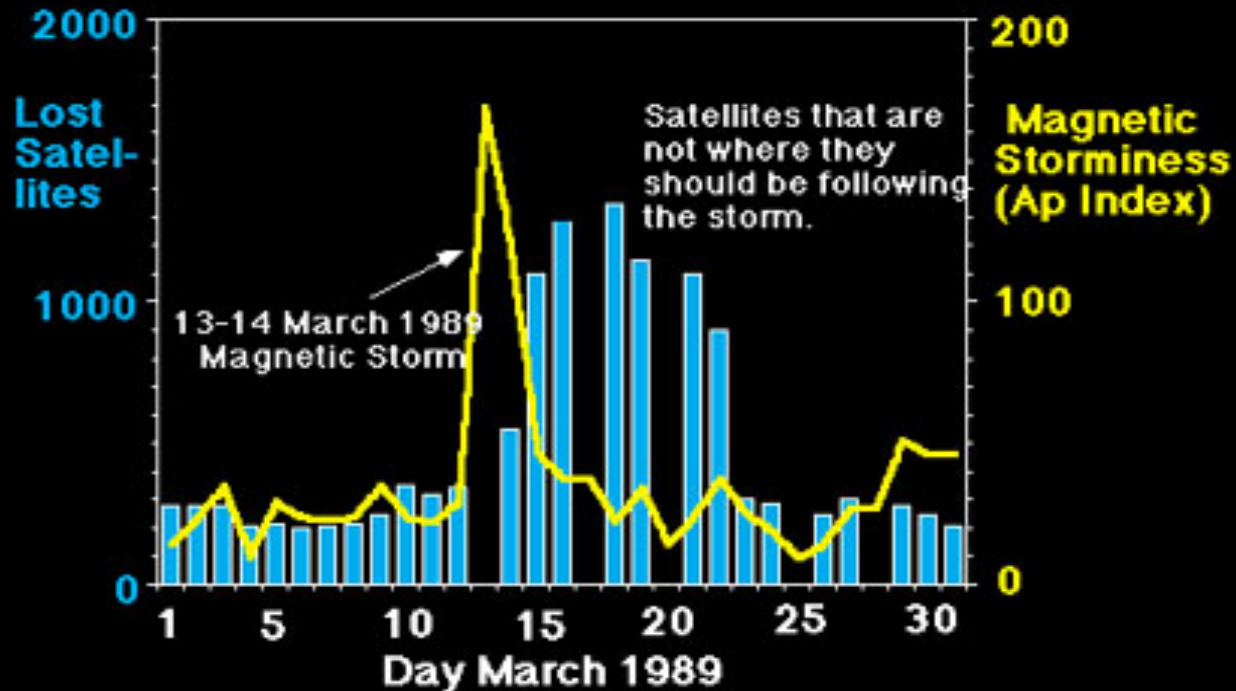
From the application to PROGRESS project that is coordinated by the University of Sheffield.

Space weather effects

1. Geomagnetically Induced Current (Power Grids, Pipelines etc)
2. Radiation effects on modern technological systems and human health
3. Satellite locations
4. Communication (propagation radio waves), in particular Solar Flare Radio Blackouts
5. Navigation Space debris

Effects of Space Weather Atmospheric Drag

Satellite Tracking Problems
After March 13-14, 1989 Storm



Increased activity heats up the atmosphere

scale-height increases

drag increases

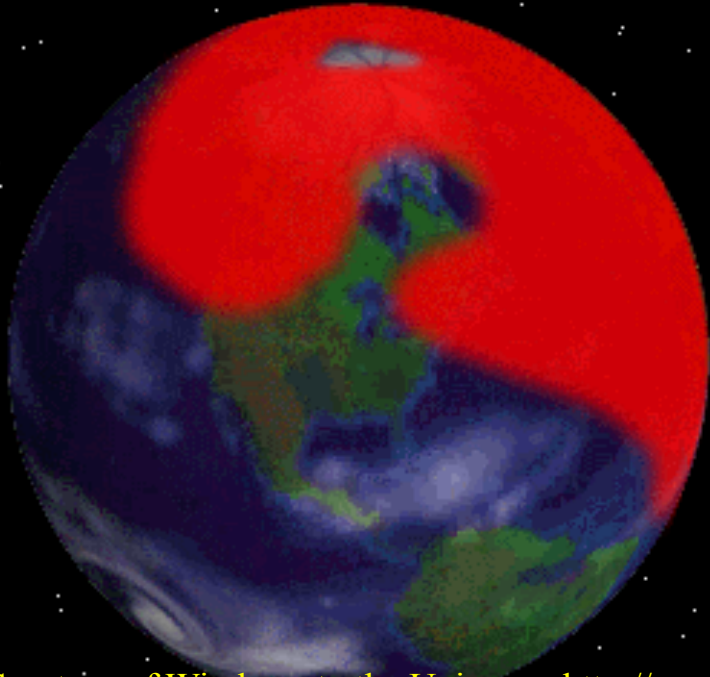
Debris and low-altitude spacecraft fall into atmosphere

Deorbiting of the MIR station to the Pacific Ocean in March 2001

”good” space weather

slowed down the natural orbital decay and the process took longer than expected

Effects of Magnetic storms Atmospheric Drag



Courtesy of Windows to the Universe, <http://www.windows.ucar.edu>

Satellites at LEO experience friction due to atmosphere.

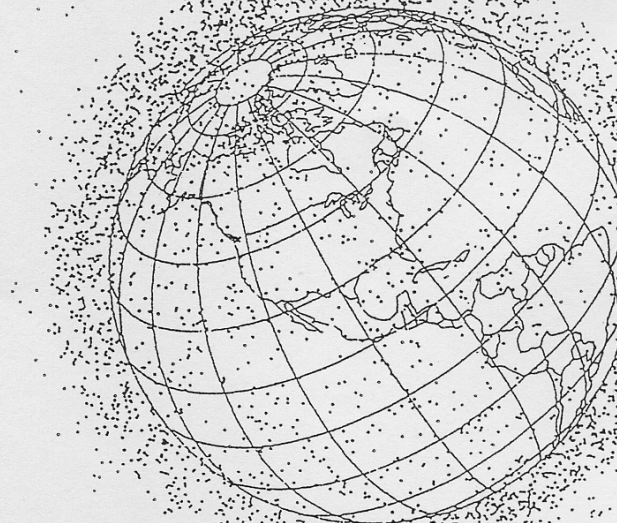
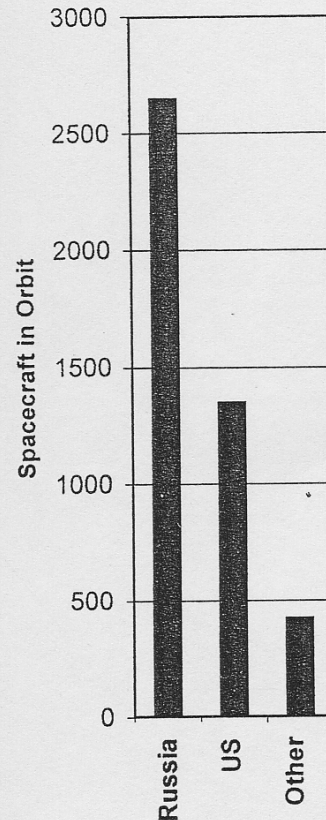
During geomagnetic disturbances electric currents increase heating and contribute to the expansion of atmosphere.

“During medium storms density of upper atmosphere increases up to 20%. The figure above illustrates such an increase. Red colour indicated area where density increase $>20\%$. During strong storms density increase can be as high as 100%. “ Windows to the Universe”

Therefore strong geomagnetic storm require re-locate the spacecraft position.

Drag and space debris

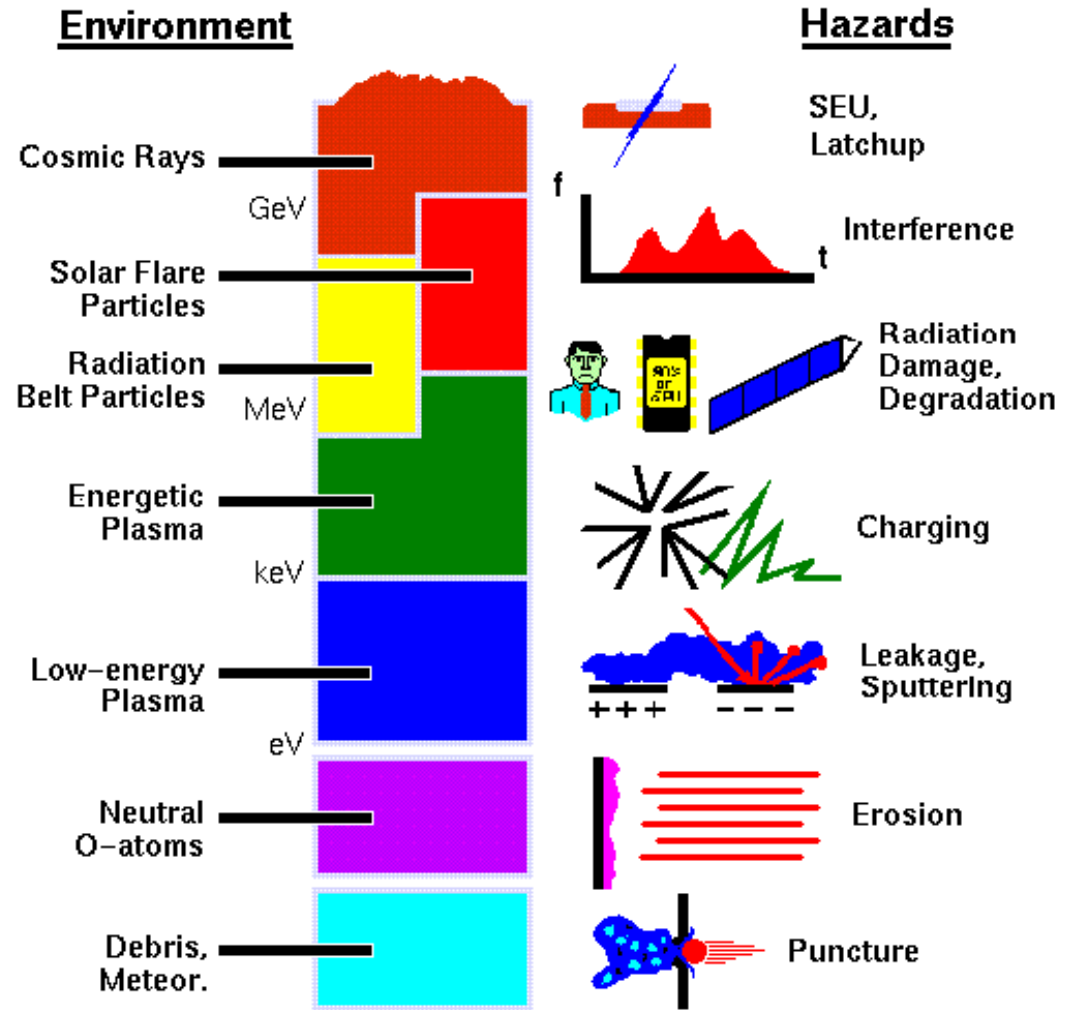
- amount of debris in space grows
 - > 10 cm bodies: > 9000
 - Hundreds of thousands smaller pieces



**1957-2001 4400
successful
spacecraft
launches.
Reference and
Image from
Charles D. Brown
Elements of
Spacecraft design,
AIAA,2002; page 3,
Fig 1.3.**

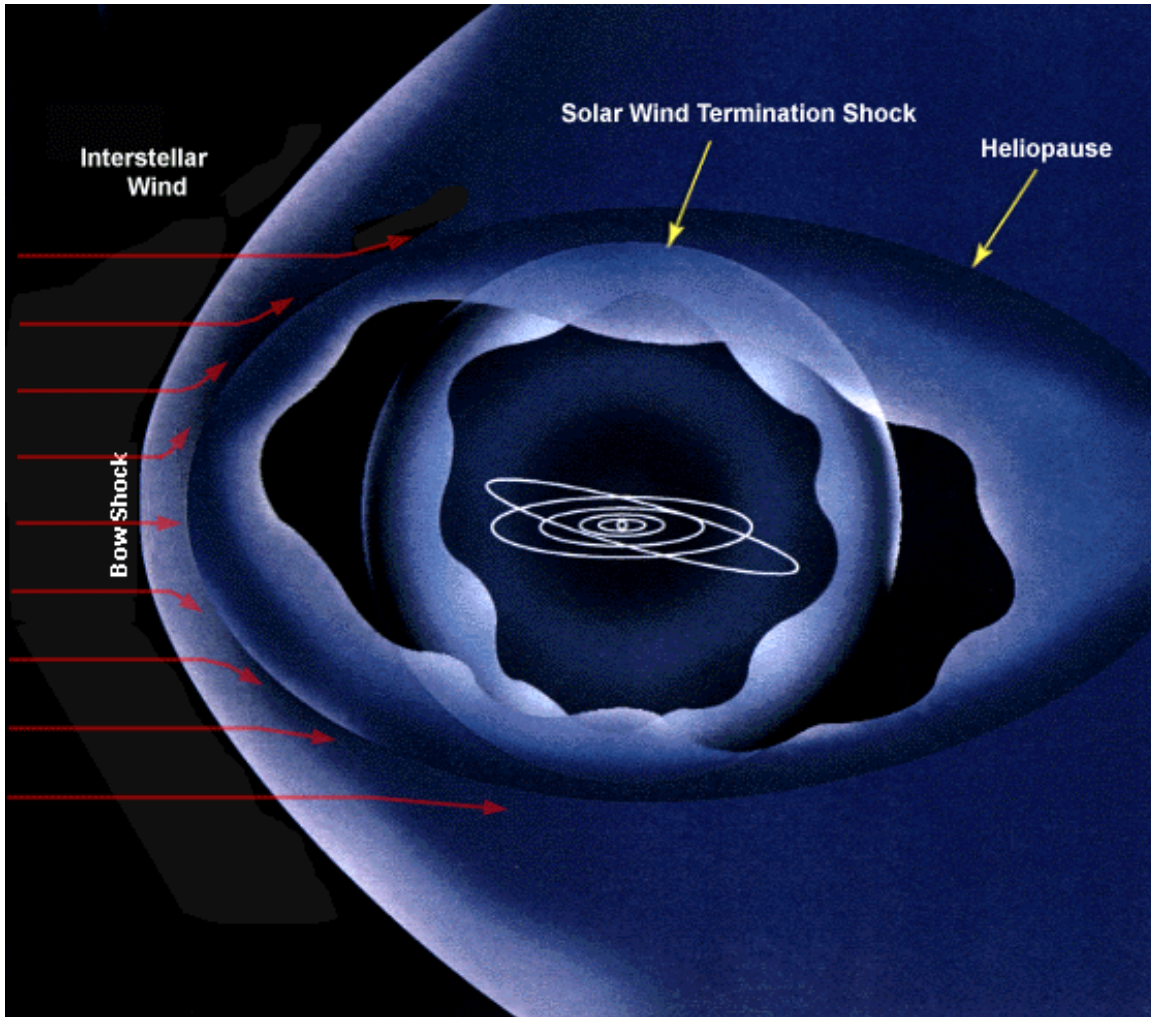
Space weather effects of particles in various energy ranges

- Dependent on:
 - particle energy
 - particle mass
 - particle flux
 - total dosage
- Effects happen:
 - on the surface
 - deep within S/C
 - in electronics
 - in biological matter



Courtesy of Dr. Ganushkina from her lecture notes

Solar wind is a shield against galactic cosmic rays



Courtesy of NASA

<https://helios.gsfc.nasa.gov/heliosphere.html>

Space Weather history: 1857

Dst: -850 nT [Baker, 2012] or -1760 nT [Tsurutani et al, 2003]

AURORAL PHENOMENA.

Remarkable Effect of the Aurora Upon the Telegraph Wires.

The Aurora which occurred on Thursday night produced effects much more remarkable than those of the previous Sunday night. The auroral currents were sufficiently powerful on Thursday to enable the telegraphic operators at Portland to transmit messages to Boston without resorting to the use of the batteries; and similar phenomena were observed at Pittsburgh. A series of experiments upon this curious electrical condition was instituted at the Boston office. The results are noticed in the Boston papers, which publish the following statements from the operators:

TELEGRAPH OFFICE, No. 31 State-street, }
Boston, Friday, Sept. 2, 1859. }

The same night the following conversation took place between the operators at the Boston and Portland offices:

Boston (to *Portland* operator)—'Please cut off your battery entirely from the line for fifteen minutes.'

Portland—'Will do so. It is now disconnected.'

Boston—'Mine is also disconnected, and we are working with the auroral current. How do you receive my writing?'

Portland—'Better than with our batteries on. Current comes and goes gradually.'

The New York Times

Published: September 5, 1859

Copyright © The New York Times

Space Weather history: May 1921

Dst: -900 [MacAlester, and Murtagh, 2014]

SUNSPOT CREDITED WITH RAIL TIE-UP

***New York Central Signal System
Put Out of Service by Play
of Northern Lights.***

The New York Times

Published: May 16, 1921

Copyright © The New York Times

CABLES DAMAGED BY SUNSPOT AURORA

**Ships to Be Sent Out to Mend
Lines Put Out of Service
by Magnetic Display.**

ASCRIBE LIGHTS TO JUPITER

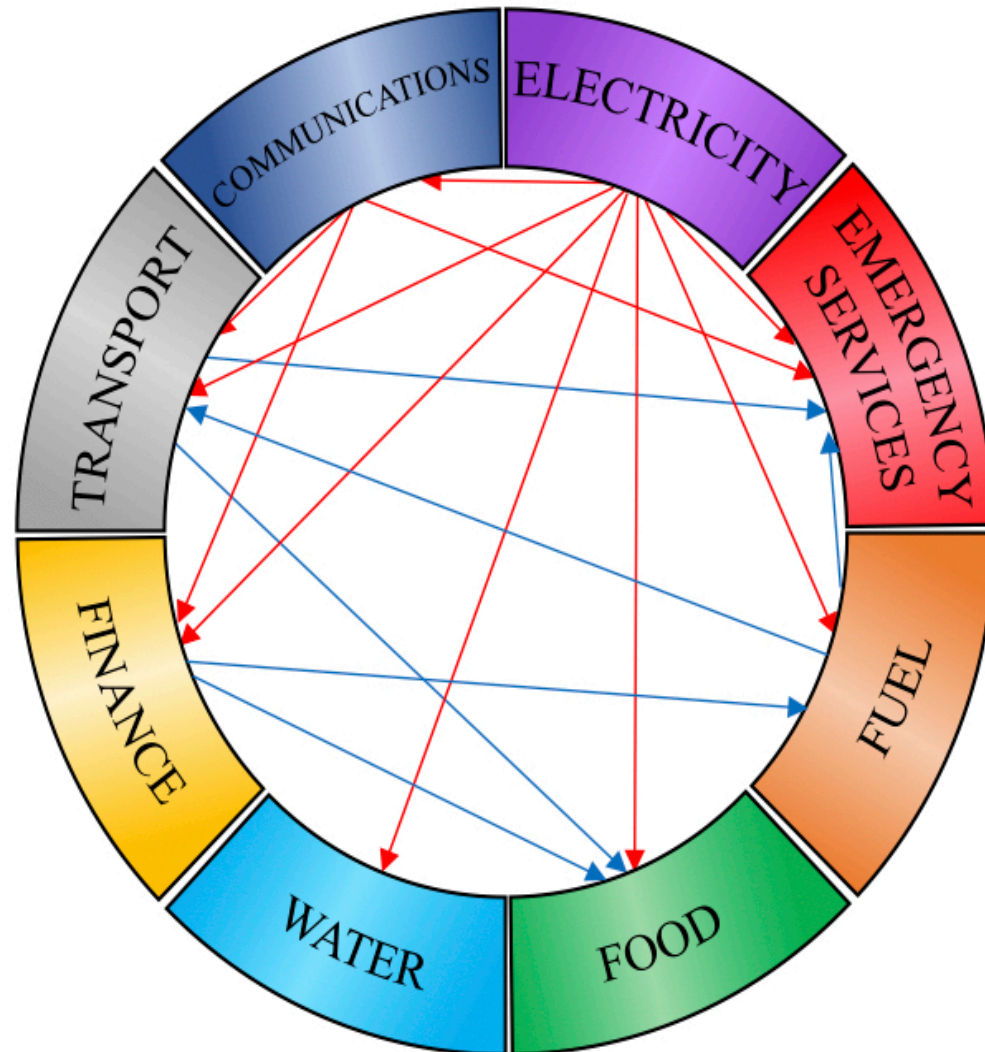
**Dr. Schlesinger of Yale Thinks
Planetary Effect on Sun May
Have Caused Disturbance.**

The New York Times

Published: May 17, 1921

Copyright © The New York Times

Space Weather Effects on Critical infrastructure



232	N24	5/18	East limb passage of one of the greatest activity complexes of Solar Cycle 20. Composed of three overlapped spot groups at time of first appearance, two of which were growing.
		5/20	Birth of fourth spot group on southern border of complex. Westward relative motion of this group, with respect to large spots to the north, may have contributed to conditions for great flare of 21 May in center of complex.
		5/21	"Collision" between central and western members of the complex, as growth and expansion of central member moved its leader spot into the follower plage of the western member. Large flare occurred over the neutral line between the groups.
		5/23	"Collision" and merger of leader of easternmost member with follower of central member, creating large "delta" magnetic configuration. Closest separation between the opposite-polarity spots coincided with great white-light, proton flare at 1840 UT (see <i>UAG Report 5</i>). These spots moved in a rotary pattern with respect to one another during 21-26 May.
a		5/28	Additional great flare over the "delta" configuration.

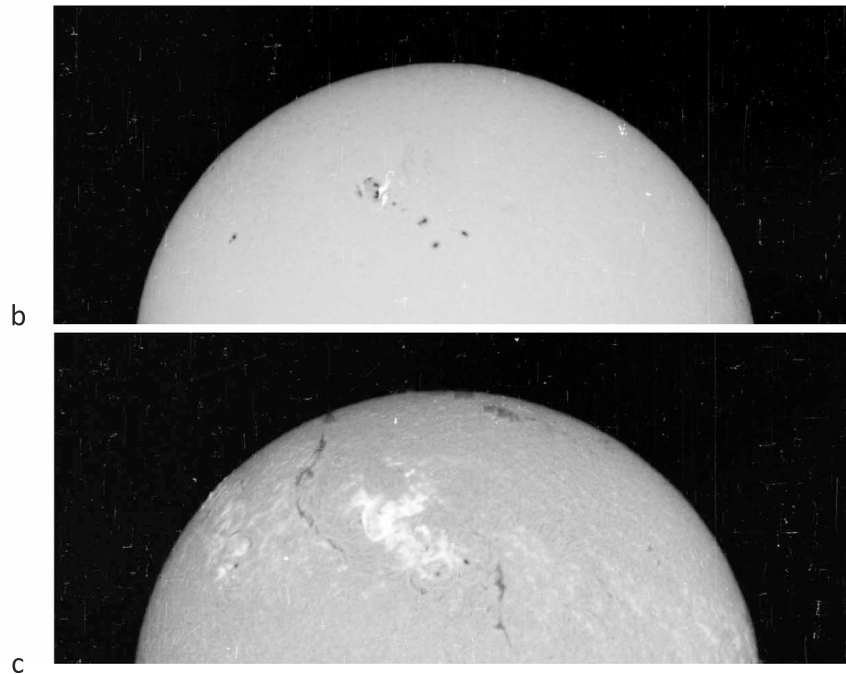


Figure From Figure (1) :
 Knipp, D. J., et al. (2016),
 Space Weather, 14, doi:
 10.1002/2016SW001423.

Figure 1. (a) Notes on the dynamics of McMath Region 8818, extracted from *McIntosh* [1979, p. 84]; (b) May 23 1967, 1840:50 UT, H α wing image, 656.28 nm, $\Delta\lambda = \pm 0.2$ nm; (c) 1844:00 UT, H α emission 656.28 nm, line center. North is at the top. West is to the right (Courtesy of National Solar Observatory).

Table 1. The 25–27 May 1967 Geomagnetic, Ionospheric, and Atmospheric Effects at 1 AU

Effect	Measurement	References
Ground magnetic and ionosphere severe storm	$Kp = 9$ for 6 h = NOAA G5 class, $Kp \geq 7$ – for 27 continuous hours, top 25 Aa_m^* storm; $Aa_m^* = 274$	NASA OMNIweb [Findlay et al., 1969; Cliver and Svalgaard, 2004]
Extreme ionospheric storm 25–26 May severe positive-negative phases	100% TEC increase on 25 May due to geomagnetic storm followed by most dominant negative phase in TEC ever recorded	Webb [1969], Low and Roelofs [1973], and Mendillo [2006]
Significant auroral precipitation effects	Scintillation on satellite beacon signal—signal lost early 25 May	Goodman [1968]
Hot ionosphere at 1000 km	Electron temperature > 6500 K, extraordinary structuring in electron density and temperature in auroral zone observed by Explorer 22 satellite	Findlay et al. [1969]
Aurora at low latitudes 25–26 May	New Mexico 32° north geographic, Alabama; overhead in Washington DC Class II aurora in Devon, UK; off-scale intensity;	Castelli et al. [1968], Findlay et al. [1969, Figure 1], and Smith and Webber [1968, Table 1]
Significant keV auroral proton precipitation 25–26 May	> 35 mW/m ² during polar pass of satellite OV1-10; 114 kR of emission	Metzger and Clark [1971]
Heated thermosphere satellite drag	400 K temperature spike after 6 h, LOGACS apogee decreases by 100 km	Jacchia [1969] and DeVries [1972]
Geomagnetic micropulsations	“Spasmodic” pulsations of 40 mV/km at 10–20 mHz	Smith and Webber [1968]
Coherent global oscillations in VLF emissions	Simultaneous global oscillations at 5–8 kHz, U.S., Europe, and Japan	Harang [1968a, 1969]
Plasmapause greatly distorted	Plasmasphere eroded to $\sim L = 2$ complex filamentary structure	Hayakawa et al. [1975] and Grebowky et al. [1974]
Dst superstorm, eighth largest 25–26 May	Sudden commencement +55 nT, Dst = –387 nT; mean $Dst_{MP} = -230$ nT, very asymmetric ring current	Kyoto Dst record [Balan et al., 2016; Akasofu et al., 1969]
Magnetospheric compressions 25–30 May	Sudden Storm Commencements (SSCs) near-equatorial ΔH of 737 nT	Lindgren [1968, Figures 6 and 9 and Table IV]
Structuring of solar energetic particle fluxes	Energetic proton enhancements ahead of and at SSC’s 24–31 May, IMP 1 and IMP 4	Lindgren [1968, Figure 4], Bostrom et al. [1969], and Lanzerotti [1969a, 1969b]
Magnetopause inside GEO orbit on May 25	> 3 h; 2039–2354 UT ATS 1 geostationary satellite	Russell [1976] and Coleman [1970]
Semipermanent disturbances in electron and proton radiation belts at $L < 3.5$	Factor of 100 increase in 0.28 MeV electrons at $L = 2.2$, increase of 0.265 MeV protons between $L = 2.25$ and 3.25 on 25 May	Bostrom et al. [1970], Rothwell and Katz [1973], and Tomblin and Kreplin [1970]
Stepped Forbush cosmic ray decrease	11% at Deep River Observatory, Marked north-south asymmetry, Cosmic ray steaming direction reversed 25–31 May	Harang [1968b], Akasofu et al. [1969, Figure 8], and Lindgren [1968]

Table From : Knipp, D. J., et al. (2016), Space Weather, 14, doi: 10.1002/2016SW001423

“Cold War military commanders viewed full scale jamming of surveillance sensors as a potential act of war” (Knipp, D. J., et al. (2016), Space Weather, 14, doi: 10.1002/2016SW001423)

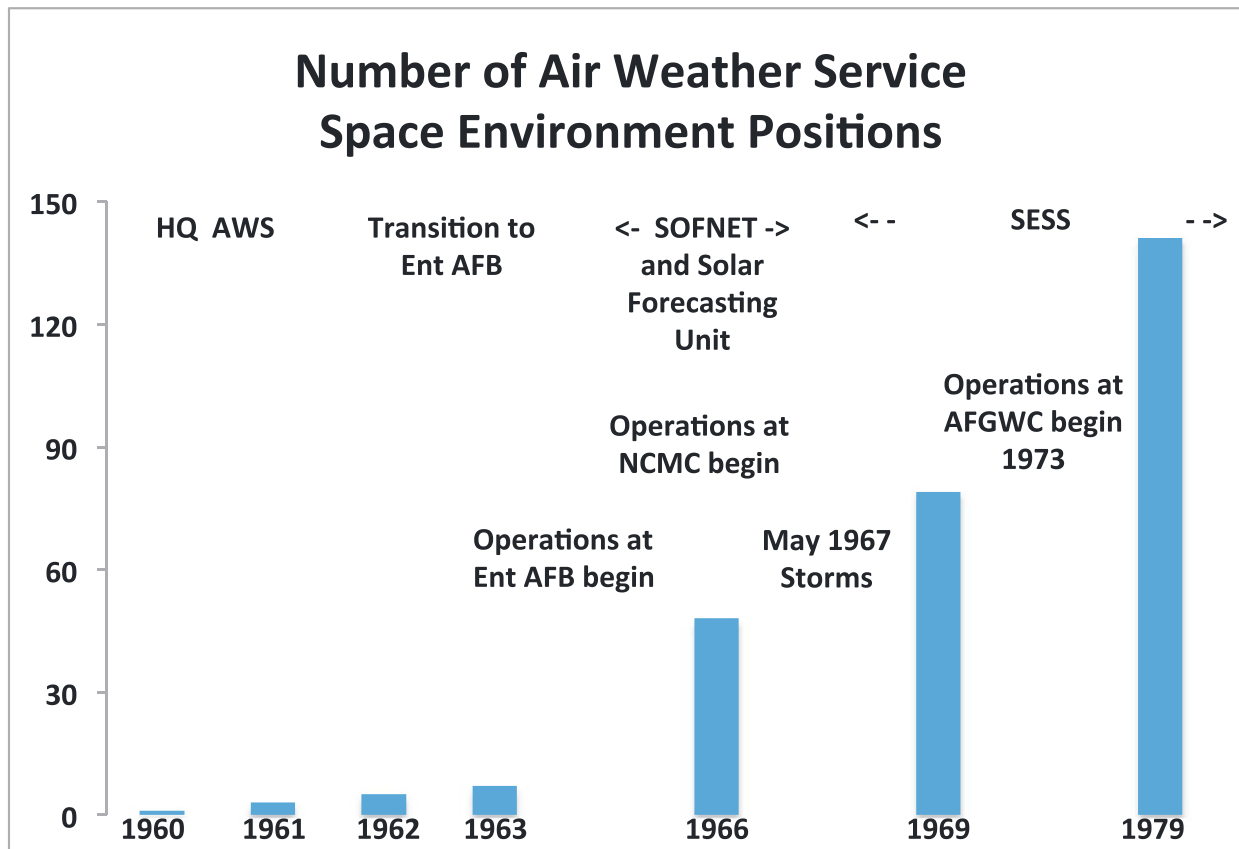
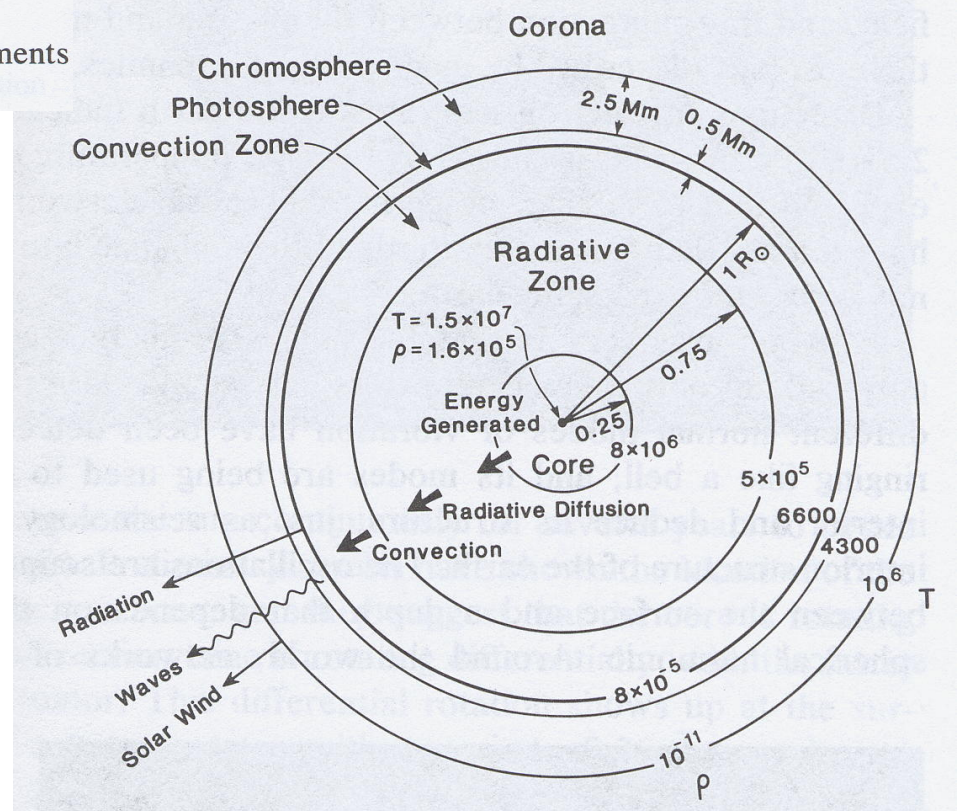


Figure 7. Number of active duty AWS Space Environment Support Positions. These numbers are taken from historical reports and rosters as well as the online AWS history. Values have an uncertainty of about 20% given that military members were often reassigned on short notice and some performed both SESS and non-SESS duties.

Sun

Age = 4.5×10^9 yr
 Mass = 1.99×10^{30} kg
 Radius = 696,000 km (696 Mm)
 Mean density = $1.4 \times 10^3 \text{ kg} \cdot \text{m}^{-3}$ ($1.4 \text{ g} \cdot \text{cm}^{-3}$)
 Mean distance from earth (1 AU) = 150×10^6 km (215 solar radii)
 Surface gravity = $274 \text{ m} \cdot \text{s}^{-2}$
 Escape velocity at surface = $618 \text{ km} \cdot \text{s}^{-1}$
 Radiation emitted (luminosity) = 3.86×10^{26} W (3.86×10^{33} erg \cdot s $^{-1}$)
 Equatorial rotation period = 26 days
 Mass loss rate = $10^9 \text{ kg} \cdot \text{s}^{-1}$
 Effective blackbody temperature = 5,785K
 Inclination of sun's equator to plane of earth's orbit = 7°
 Composition: approximately 90% H, 10% He, 0.1% other elements
 (C, N, O, . . .)



From : Kivelson, M. and C. T. Russell eds, Introduction to Space Physics, Cambridge University Press, 1995.

Solar Cycle

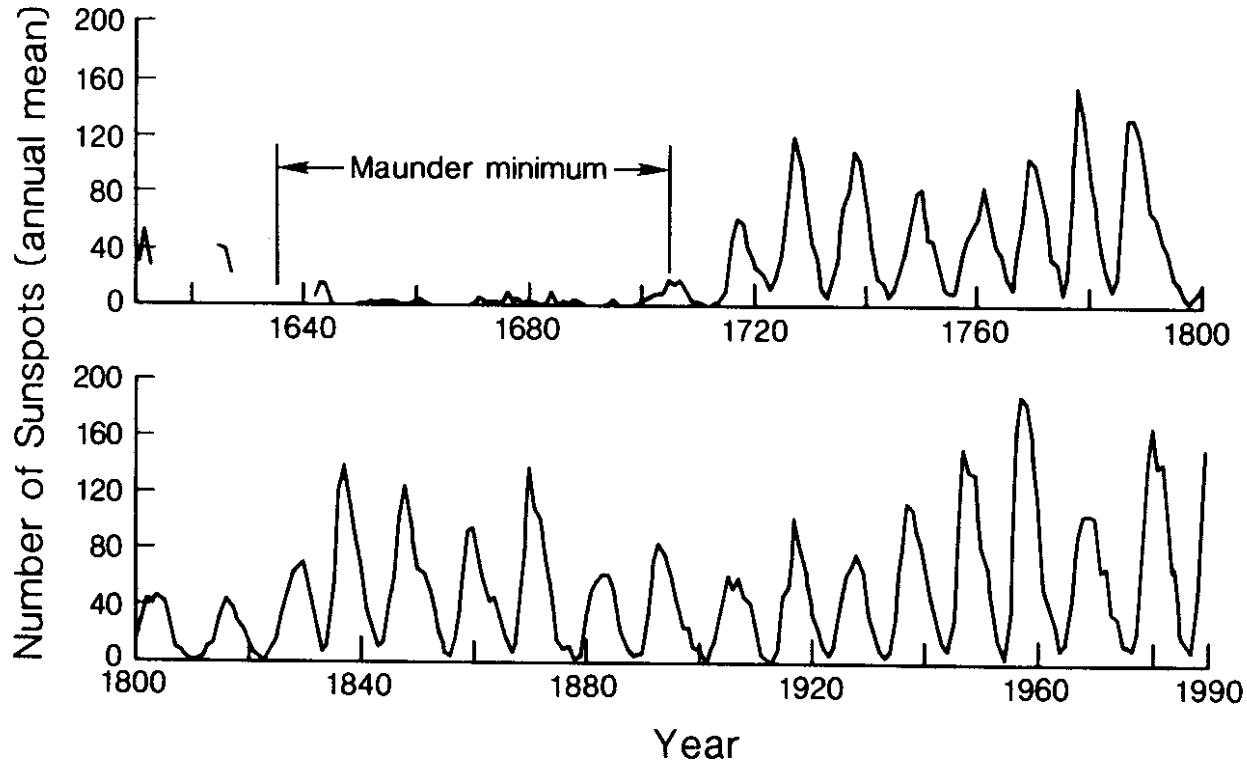


Figure : Kivelson, M. and C. T. Russell eds, Introduction to Space Physics, Cambridge University Press, 1995.

Solar wind

Solar Wind parameters In the vicinity of the Earth

Electron density	7 cm^{-3}
Solar Wind speed	450km/s
Proton temperature	120,000
degrees. 11eV	
Electron temperature	135,000
degrees. 12eV	
Magnetic Field	$7 \times 10^{-9} \text{ T} = 7 \text{ nT}$

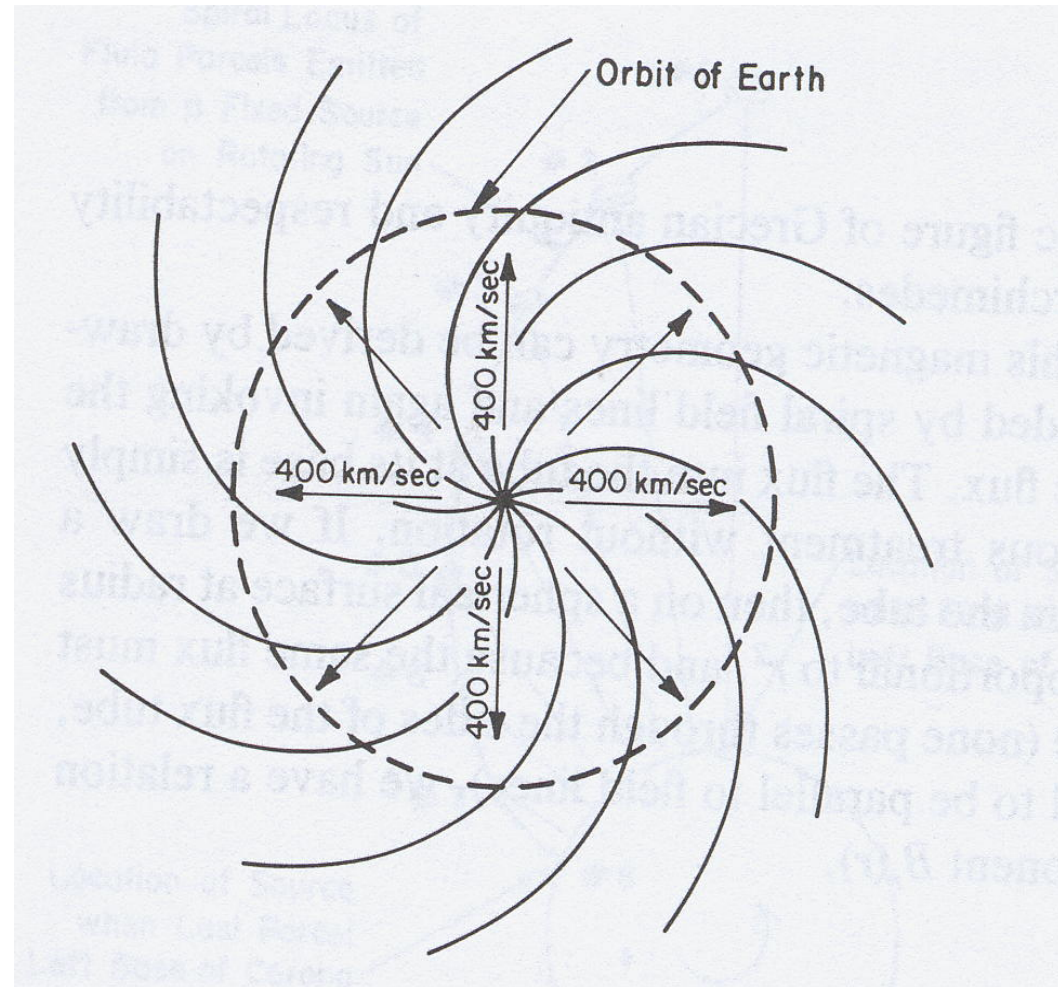
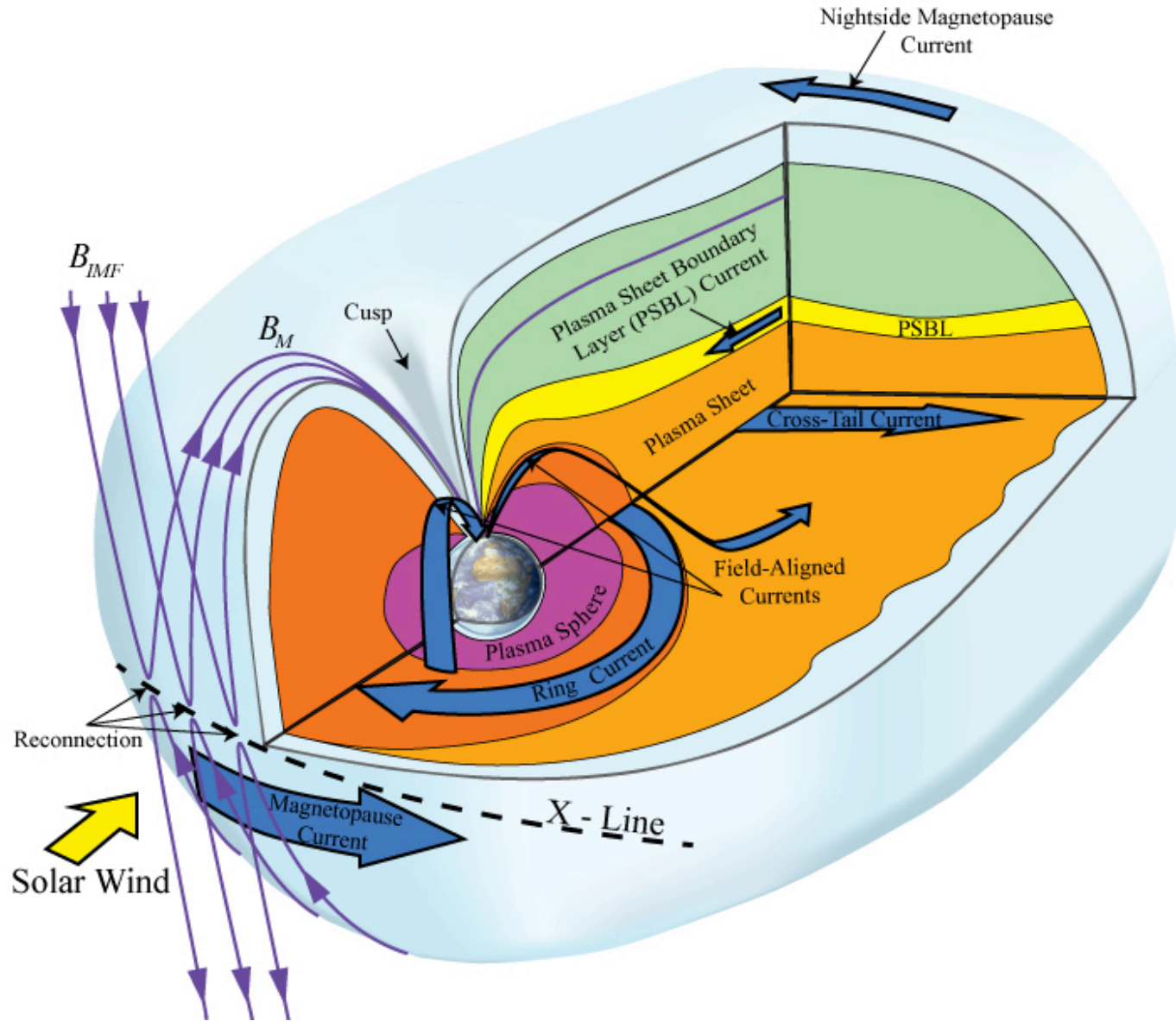


Figure From : Kivelson, M. and C. T. Russell eds,
Introduction to Space Physics, Cambridge University
Press, 1995.

Terrestrial environment



Effects of Space Weather :

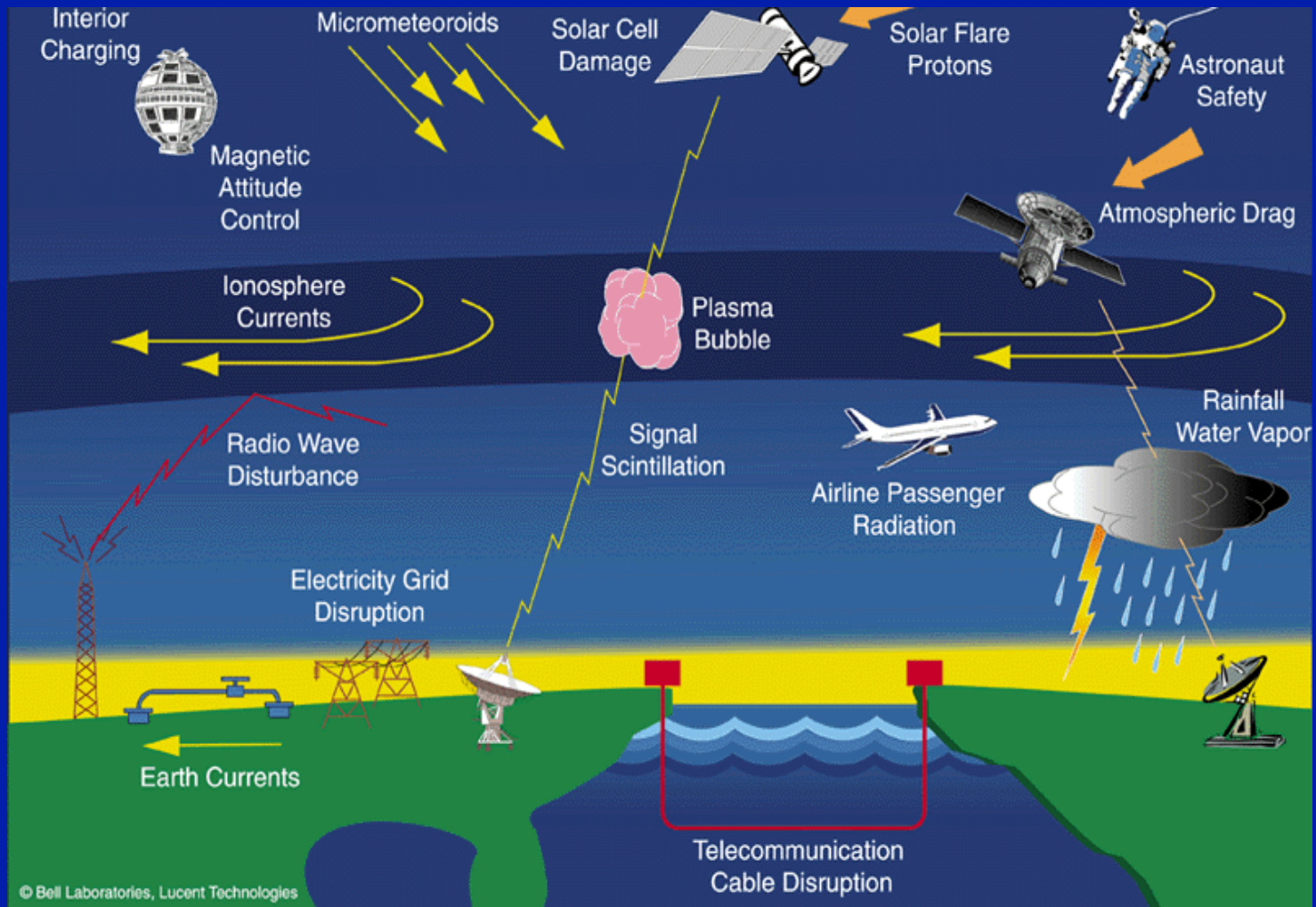


Image credit: Lanzeroti LJ Bell laboratories, Lucent Technologies incorporation

Effects of Space Weather : Ground Induced Currents (GIC)

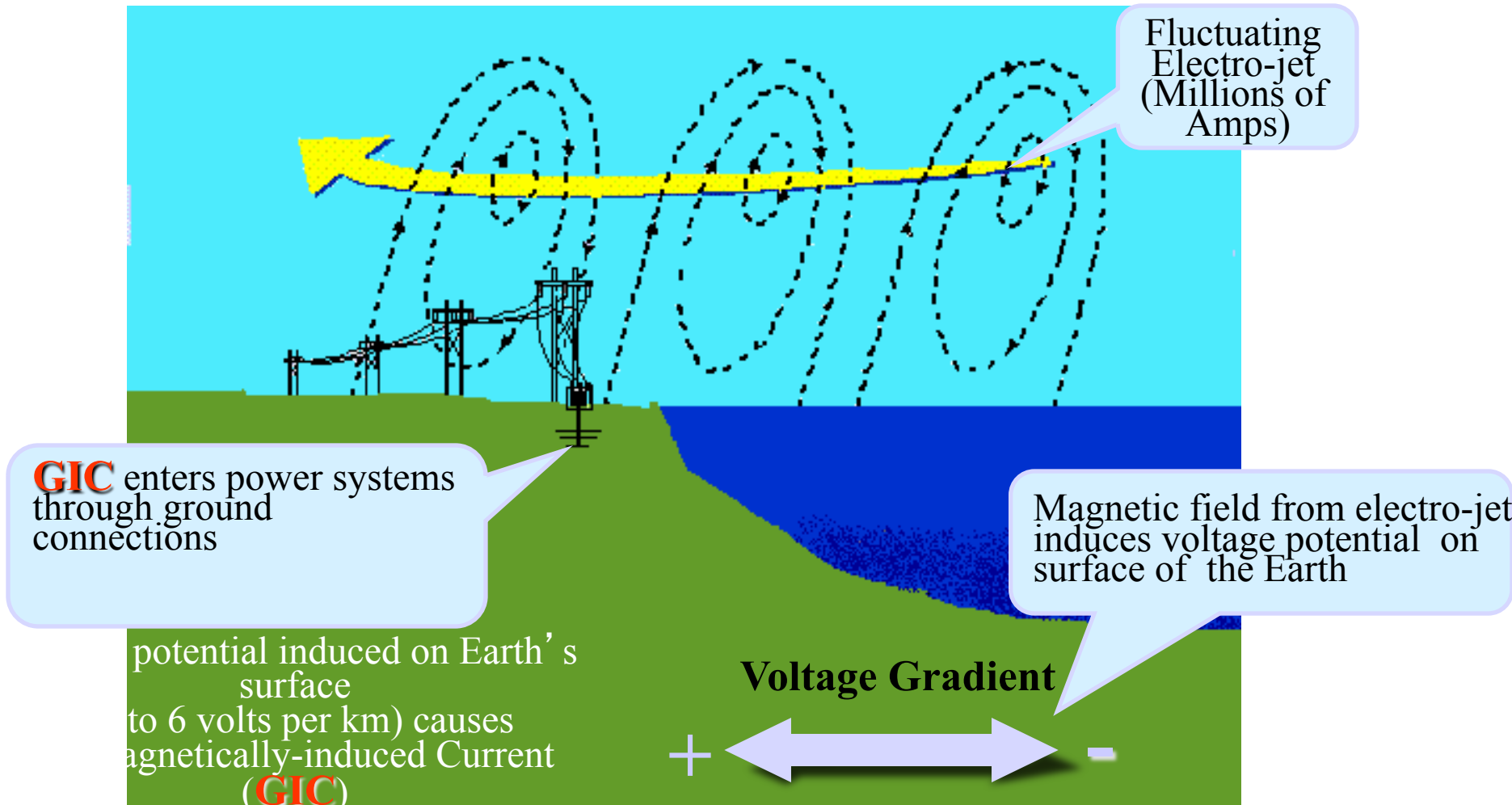


Image from <https://earthchangesmedia.wordpress.com/2015/08/24/new-study-finds-earths-equatorial-regions-prone-to-disruptive-space-weather/>

Effects of Space Weather :

Ground Induced Currents (GIC)



Power Grids

Effect:

Superposition of DC GIC and AC current leads under extreme space weather conditions to failures of transformers

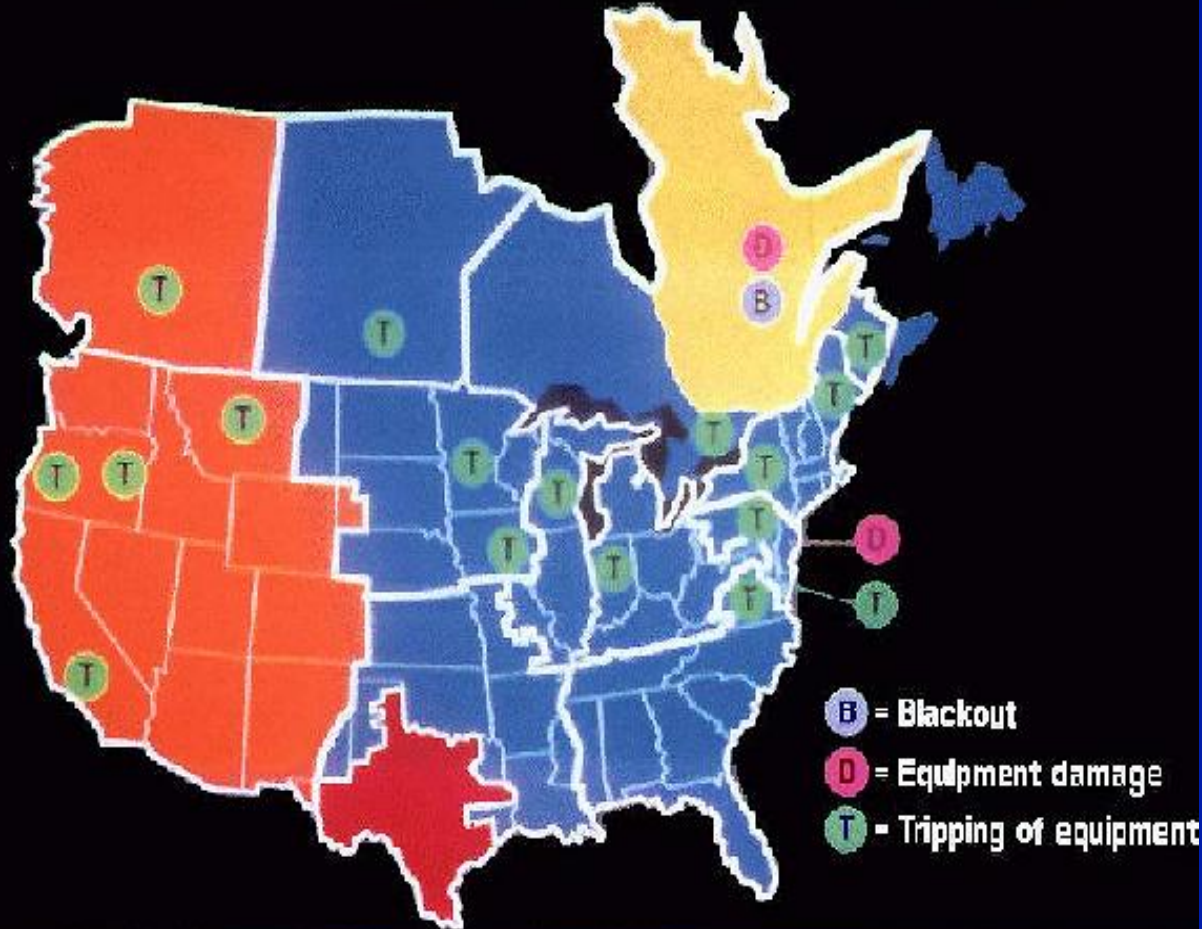
Pipelines

Transoceanic cables

Image from http://science.nasa.gov/science-news/science-at-nasa/2010/26oct_solarshield/
Permanent damage to the Salem New Jersey Nuclear Plant GSU Transformer caused by the March 13, 1989 geomagnetic storm. Photos courtesy of PSE&G.

Effects of Space Weather : Ground Induced Currents (GIC)

POWER SYSTEM EVENTS DUE TO SMD MARCH 13, 1989



Power Grids

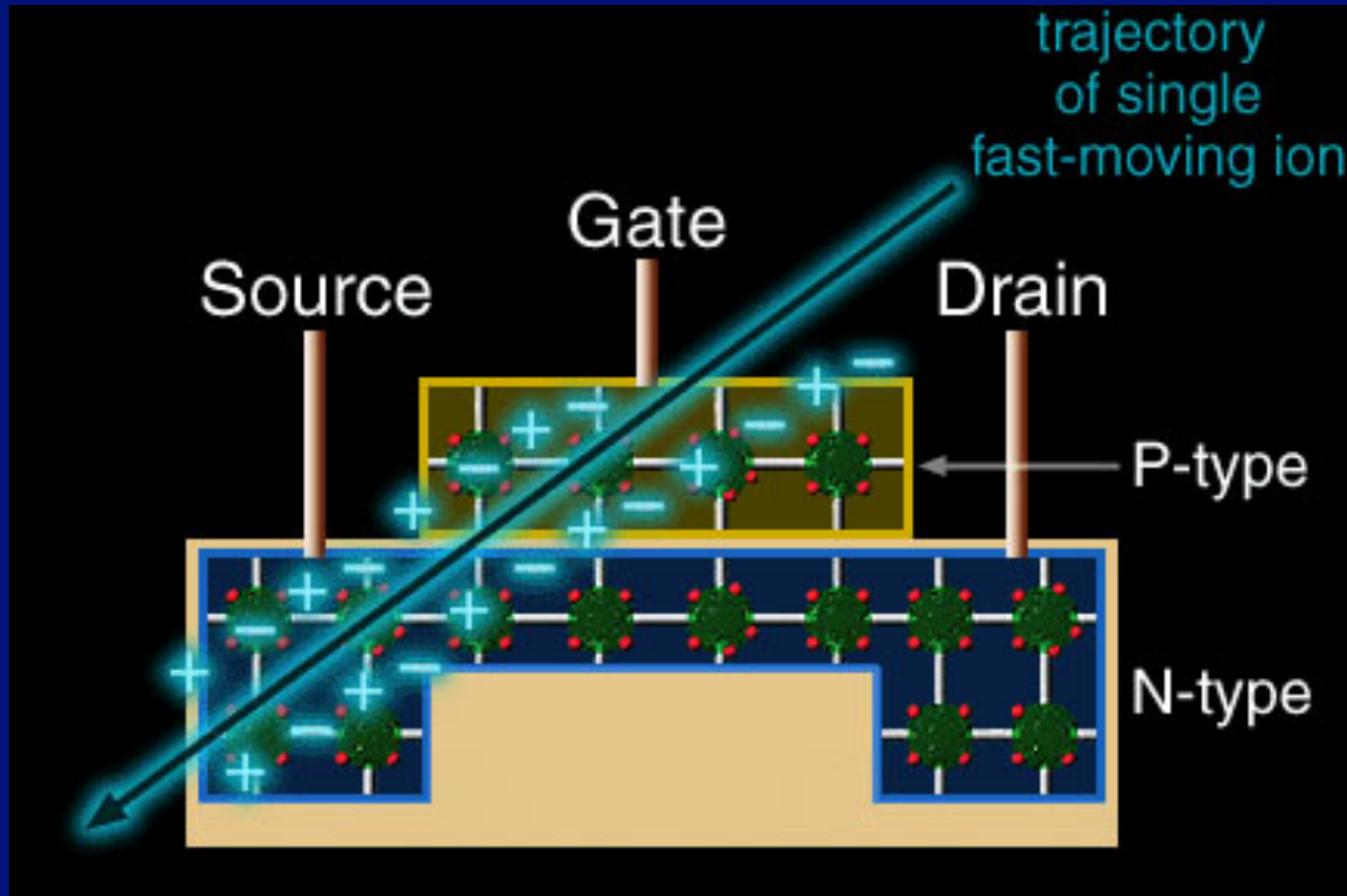
Effect:
Superposition of DC GIC and AC current leads under extreme space weather conditions to failures of transformers (Quebec Blackout)

Pipelines

Transoceanic cables

Effects of Space Weather: Radiation

Damage to solar cell



Energetic particles damage solar arrays.

Radiation Belts

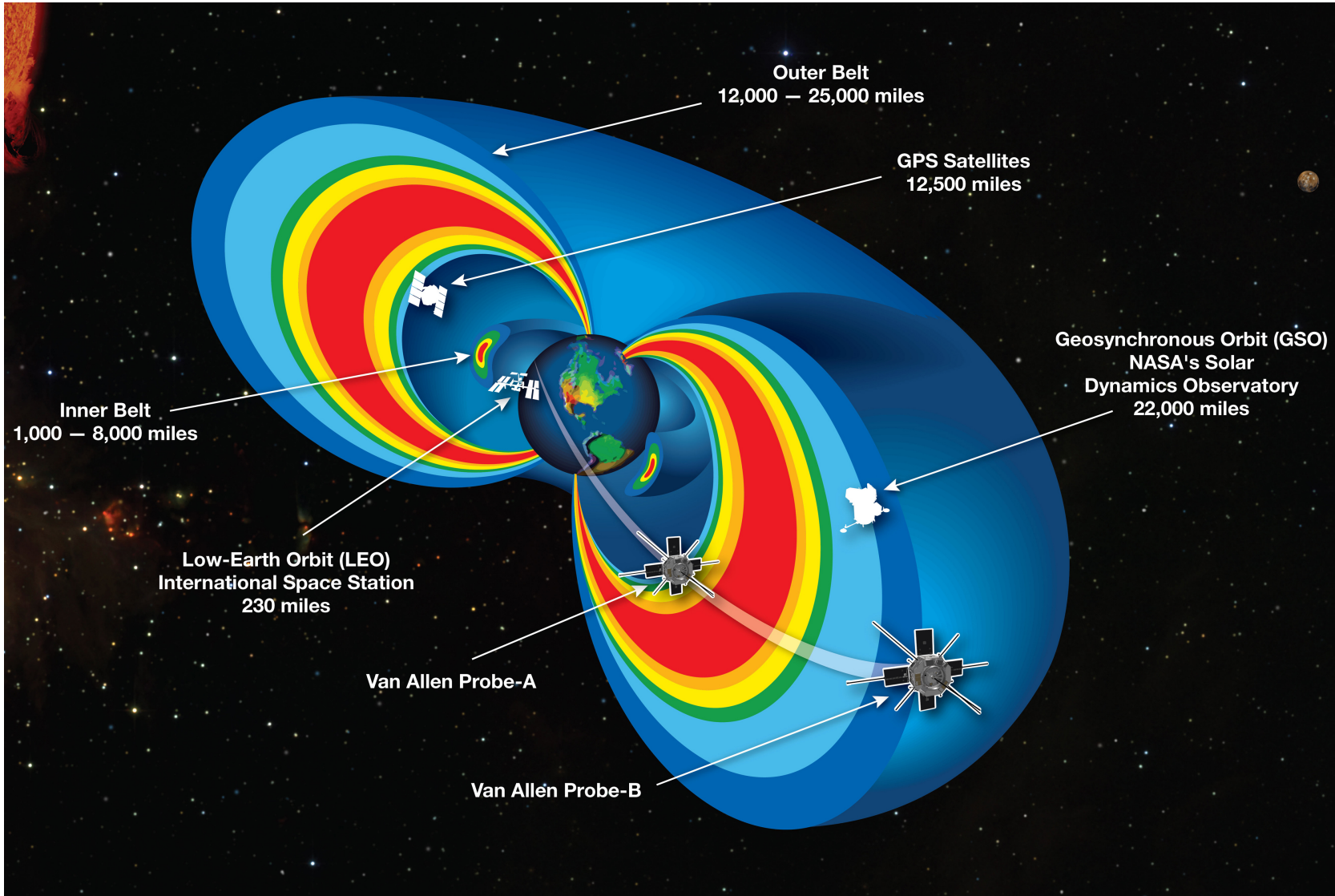
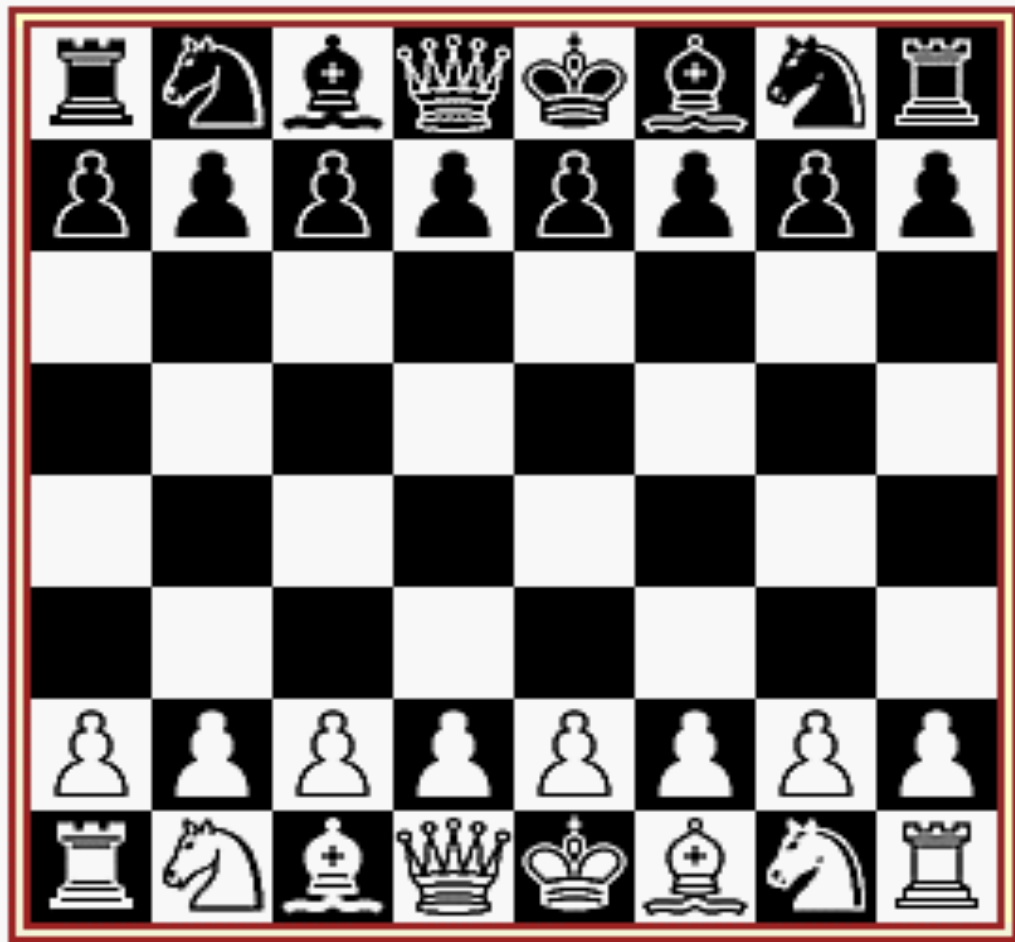


Image credit: NASA

http://www.nasa.gov/sites/default/files/images/730056main_20130228-radiationbelts-orig_full.jpg

Effects of energetic electrons in The outer radiation belt

1. Internal charging (high energy electrons)
2. Surface charging (low energy electrons)
3. Damage to solar panels
4. Single events upsets



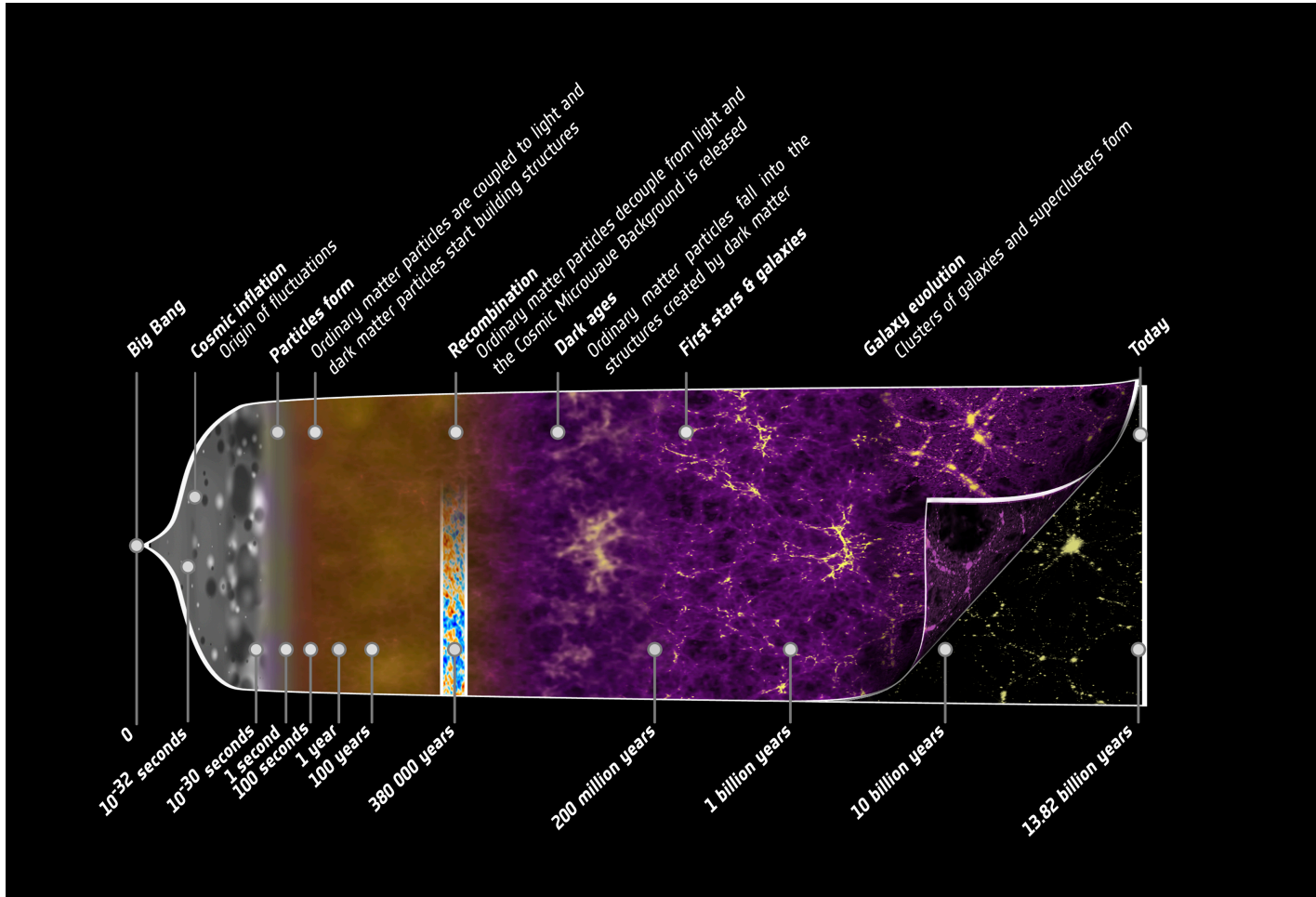


Image courtesy ESA
 Copyright ESA – C. Carreau
http://www.esa.int/spaceinimages/Images/2013/03/Planck_history_of_Universe_zoom

Homogeneous time

$$S(q) = \int_{t_1}^{t_2} L(q(t), \dot{q}(t), t) dt \quad c = \text{constant}$$



System Identification Approach

Analytical Approach

$$S = \int L(x, \dot{x}, t) dt$$
$$dL = \sum_i \frac{\partial L}{\partial x_i} dx_i + \sum_i \frac{\partial L}{\partial \dot{x}_i} d\dot{x}_i$$



Assumptions

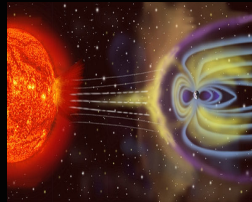
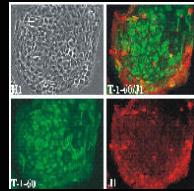
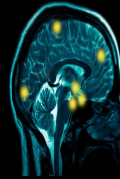


Physical Knowledge



First Principles

Black box System



Systems Approach

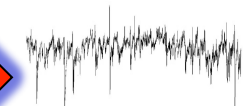
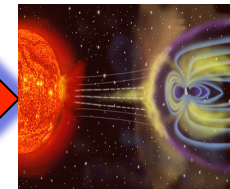
Physical Knowledge of the System



$$S = \int L(x, \dot{x}, t) dt$$
$$dL = \sum_i \frac{\partial L}{\partial x_i} dx_i + \sum_i \frac{\partial L}{\partial \dot{x}_i} d\dot{x}_i$$



Input Data



Output Data

“Physics” based versus data based forecasts

First Principles based forecast

$$S = \int L(x, \dot{x}, t) dt$$
$$dL = \sum_i \frac{\partial L}{\partial x_i} dx_i + \sum_i \frac{\partial L}{\partial \dot{x}_i} d\dot{x}_i$$



Assumptions



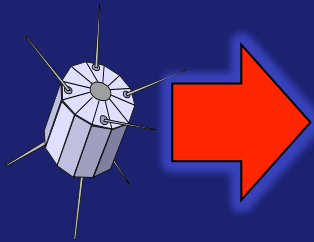
Physical
Knowledge



First Principles

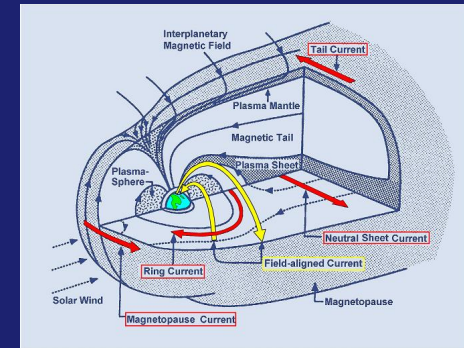
“Physics” based versus data based forecast

First Principles based forecast



L1

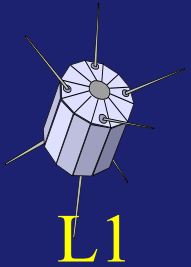
$$S = \int L(x, \dot{x}, t) dt$$
$$dL = \sum_i \frac{\partial L}{\partial x_i} dx_i + \sum_i \frac{\partial L}{\partial \dot{x}_i} d\dot{x}_i$$



Forecast

“Physics” based versus data based forecast

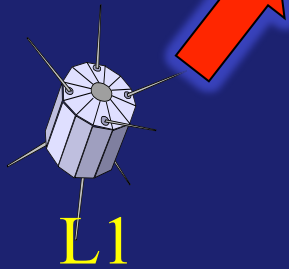
First Principles based forecast of high energy fluxes of
Radiation belts



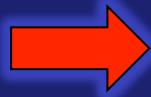
Forecast

“Physics” based versus data based forecast

First Principles based forecast of high energy fluxes of
Radiation belts



$$S = \int L(x, x, t) dt$$
$$dL = \sum_i \frac{\partial L}{\partial x_i} dx_i + \sum_i \frac{\partial L}{\partial \dot{x}_i} d\dot{x}_i$$

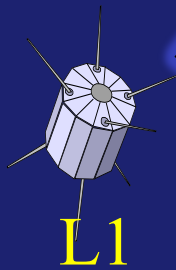


Boundary
conditions

Forecast

“Physics” based versus data based forecast

First Principles based forecast of high energy fluxes of Radiation belts

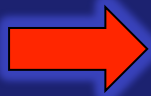


$$S = \int L(x, x, \dot{x}, t) dt$$
$$dL = \sum_i \frac{\partial L}{\partial x_i} dx_i + \sum_i \frac{\partial L}{\partial \dot{x}_i} d\dot{x}_i$$



Boundary
conditions

$$S = \int L(x, x, \dot{x}, t) dt$$
$$dL = \sum_i \frac{\partial L}{\partial x_i} dx_i + \sum_i \frac{\partial L}{\partial \dot{x}_i} d\dot{x}_i$$

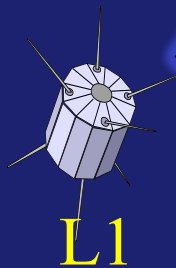


Model of the
magnetic field

Forecast

“Physics” based versus data based forecast

First Principles based forecast of high energy fluxes of Radiation belts



$$S = \int L(x, x, t) dt$$
$$dL = \sum_i \frac{\partial L}{\partial x_i} dx_i + \sum_i \frac{\partial L}{\partial \dot{x}_i} d\dot{x}_i$$

Boundary
conditions

$$S = \int L(x, x, t) dt$$
$$dL = \sum_i \frac{\partial L}{\partial x_i} dx_i + \sum_i \frac{\partial L}{\partial \dot{x}_i} d\dot{x}_i$$

Model of the
magnetic field

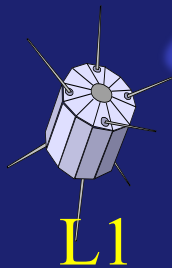
$$S = \int L(x, x, t) dt$$
$$dL = \sum_i \frac{\partial L}{\partial x_i} dx_i + \sum_i \frac{\partial L}{\partial \dot{x}_i} d\dot{x}_i$$

Wave model for
the distribution of
Hiss, Chorus,
EMW, EMIC

Forecast

“Physics” based versus data based forecast

First Principles based forecast of high energy fluxes of Radiation belts



$$S = \int L(x, x, t) dt$$
$$dL = \sum_i \frac{\partial L}{\partial x_i} dx_i + \sum_i \frac{\partial L}{\partial \dot{x}_i} d\dot{x}_i$$

Boundary conditions

$$S = \int L(x, x, t) dt$$
$$dL = \sum_i \frac{\partial L}{\partial x_i} dx_i + \sum_i \frac{\partial L}{\partial \dot{x}_i} d\dot{x}_i$$

$$S = \int L(x, x, t) dt$$
$$dL = \sum_i \frac{\partial L}{\partial x_i} dx_i + \sum_i \frac{\partial L}{\partial \dot{x}_i} d\dot{x}_i$$

Model of the magnetic field

$$S = \int L(x, x, t) dt$$
$$dL = \sum_i \frac{\partial L}{\partial x_i} dx_i + \sum_i \frac{\partial L}{\partial \dot{x}_i} d\dot{x}_i$$

Forecast

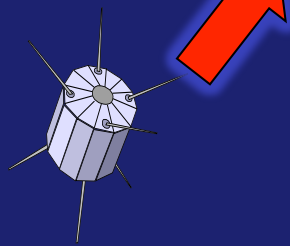
$$S = \int L(x, x, t) dt$$
$$dL = \sum_i \frac{\partial L}{\partial x_i} dx_i + \sum_i \frac{\partial L}{\partial \dot{x}_i} d\dot{x}_i$$

Wave model for the distribution of Hiss, Chorus, EMW, EMIC

$$S = \int L(x, x, t) dt$$
$$dL = \sum_i \frac{\partial L}{\partial x_i} dx_i + \sum_i \frac{\partial L}{\partial \dot{x}_i} d\dot{x}_i$$

“Physics” based versus data based forecast

First Principles based forecast of high energy fluxes of
Radiation belts



$$S = \int L(x, x, t) dt$$
$$dL = \sum_i \frac{\partial L}{\partial x_i} dx_i + \sum_i \frac{\partial L}{\partial \dot{x}_i} d\dot{x}_i$$

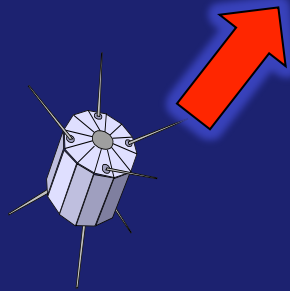


Boundary
conditions

Forecast

“Physics” based versus data based forecast

First Principles based forecast of high energy fluxes of
Radiation belts



Tsyganenko
Mukai 2003
Empirical

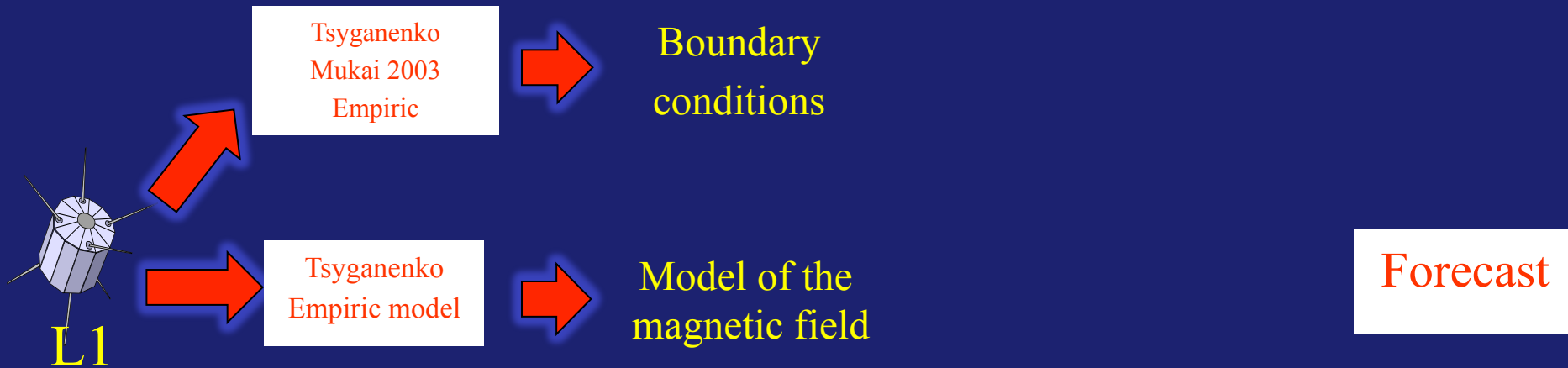


Boundary
conditions

Forecast

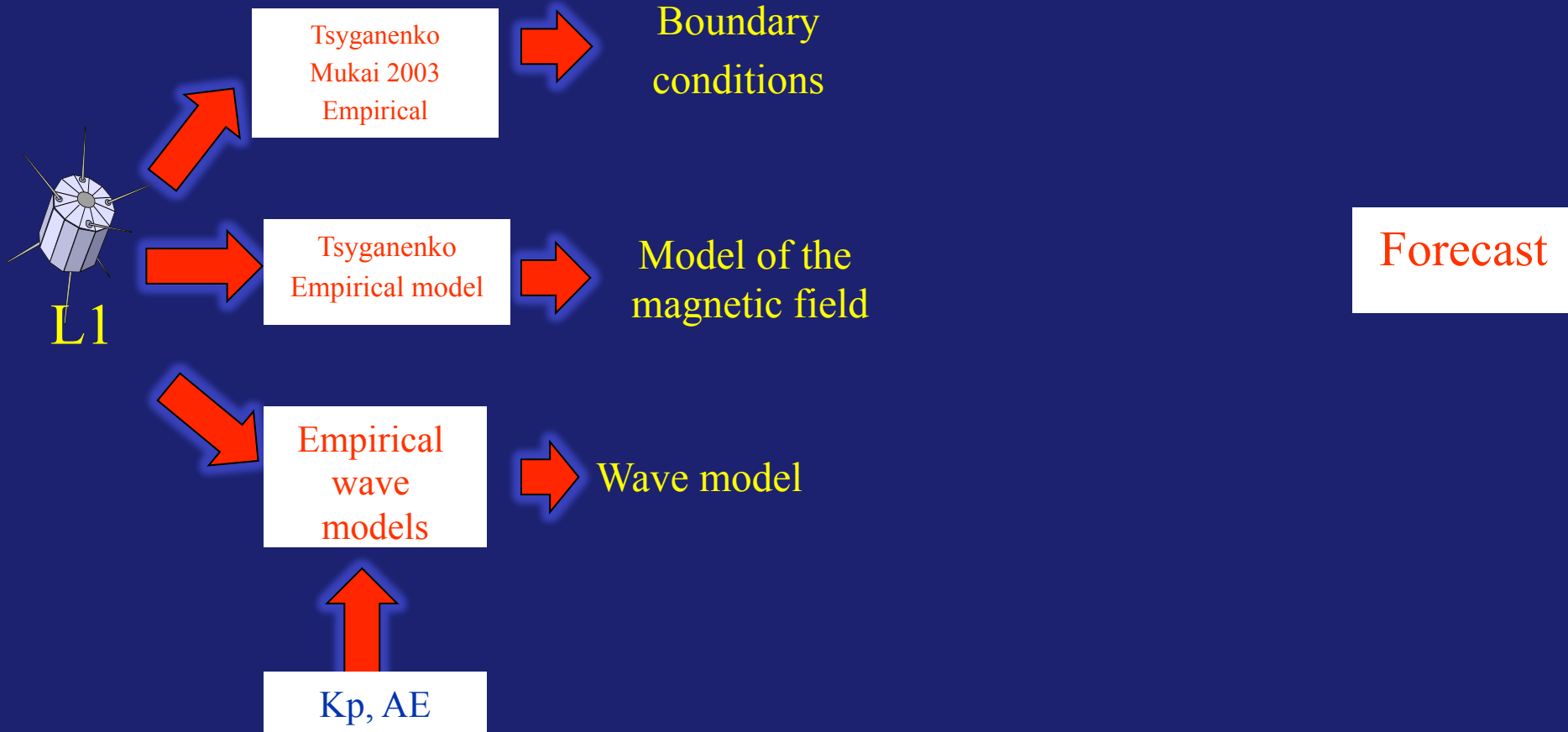
“Physics” based versus data based forecast

First Principles based forecast of high energy fluxes of
Radiation belts



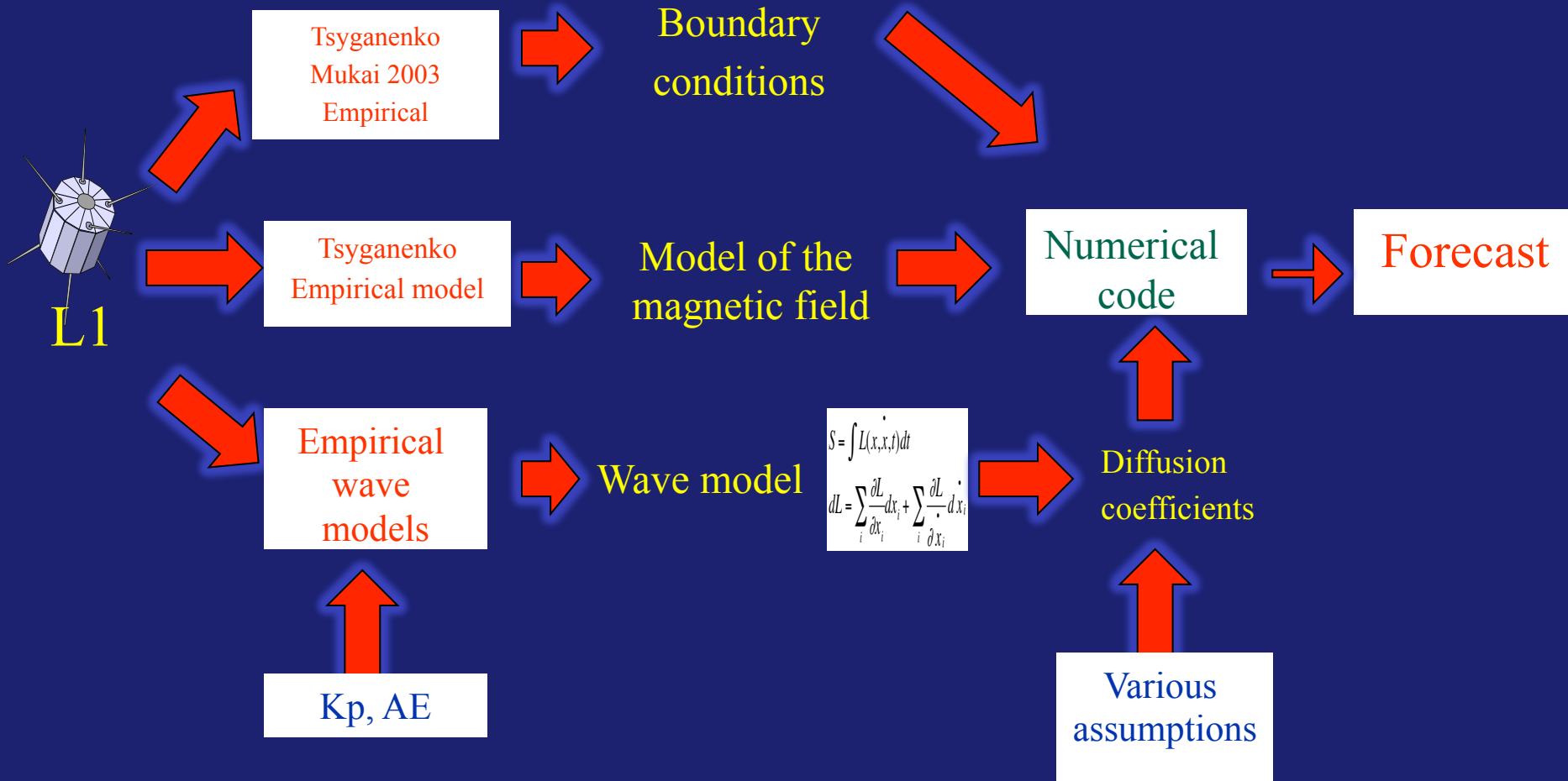
“Physics” based versus data based forecast

First Principles based forecast of high energy fluxes of
Radiation belts



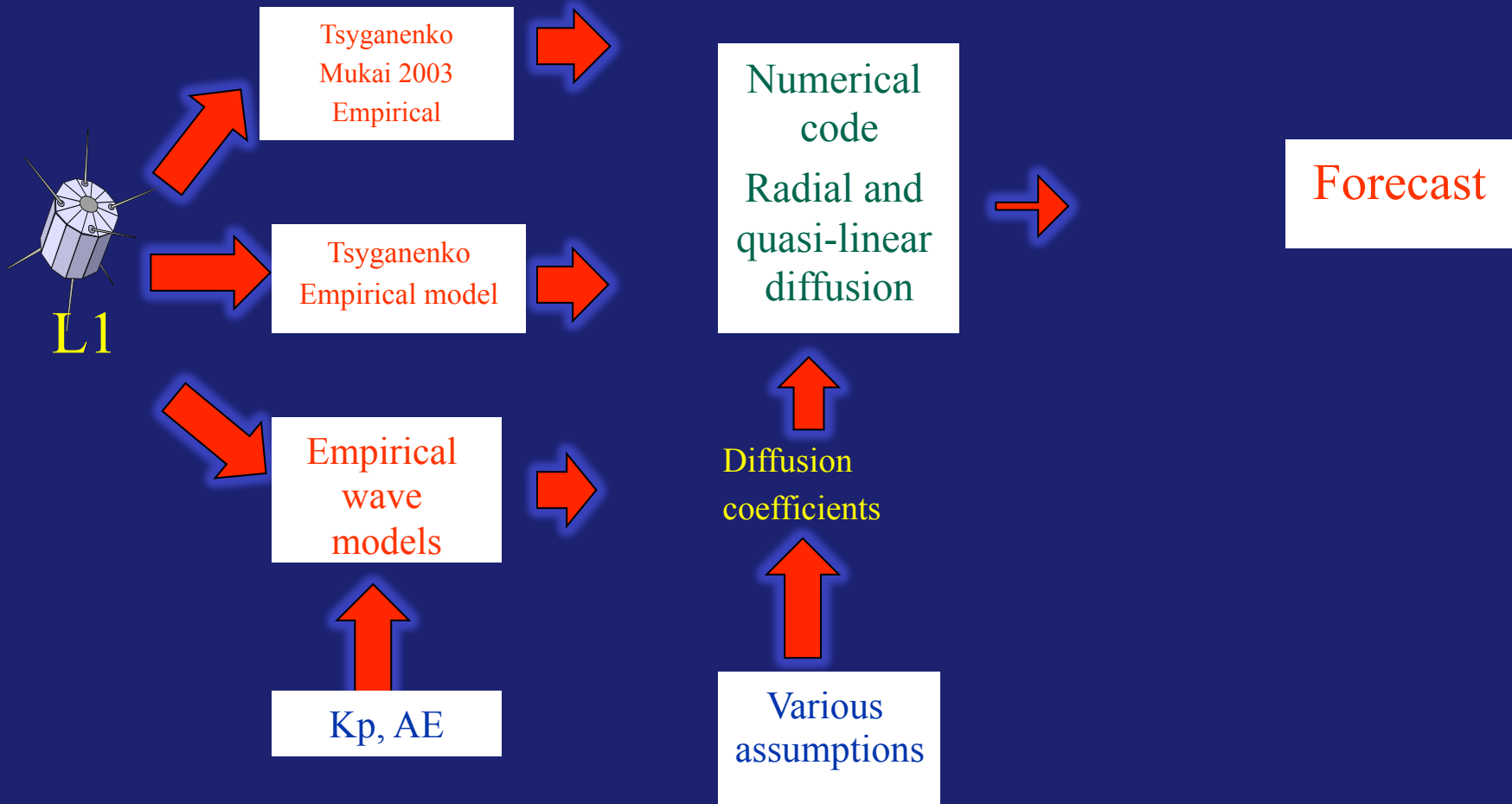
“Physics” based versus data based forecast

First Principles based forecast of high energy fluxes of Radiation belts



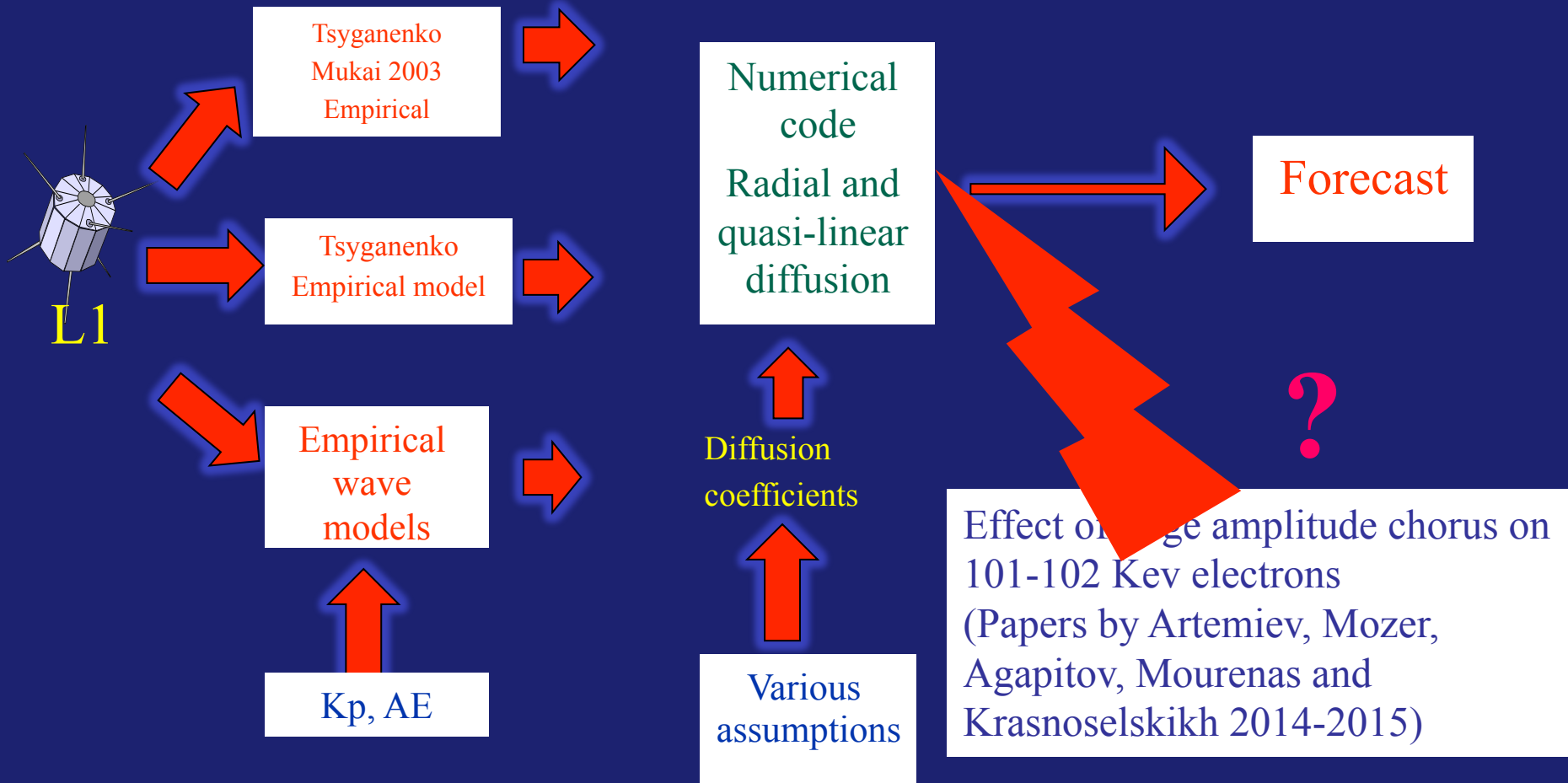
“Physics” based versus data based forecast

First Principles based forecast of high energy fluxes of
Radiation belts



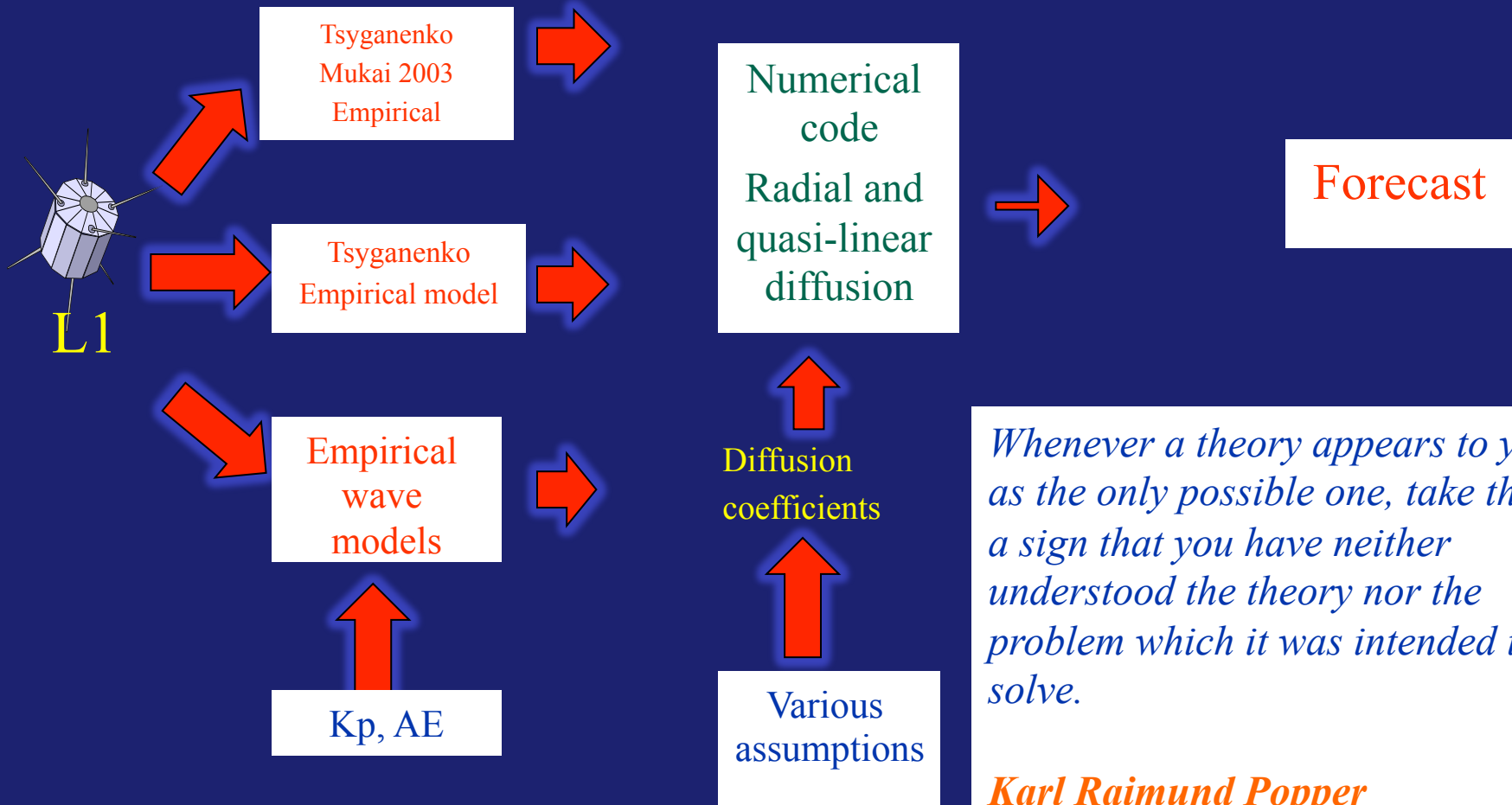
“Physics” based versus data based forecast

First Principles based forecast of high energy fluxes of Radiation belts



“Physics” based versus data based forecast

First Principles based forecast of high energy fluxes of Radiation belts



Whenever a theory appears to you as the only possible one, take this as a sign that you have neither understood the theory nor the problem which it was intended to solve.

Karl Raimund Popper

System Identification Approach

Analytical Approach

$$S = \int L(x, \dot{x}, t) dt$$

$$dL = \sum_i \frac{\partial L}{\partial x_i} dx_i + \sum_i \frac{\partial L}{\partial \dot{x}_i} d\dot{x}_i$$



Assumptions

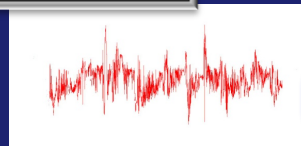
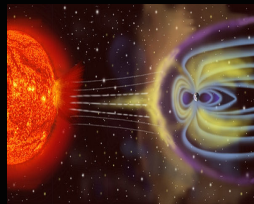
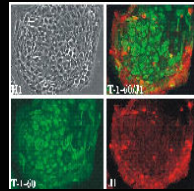


Physical Knowledge



First Principles

Black box System



Input Data

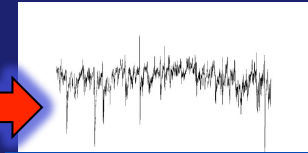
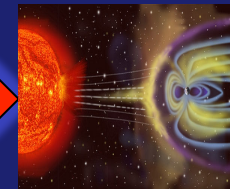
Systems Approach

Knowledge of the System



$$S = \int L(x, \dot{x}, t) dt$$

$$dL = \sum_i \frac{\partial L}{\partial x_i} dx_i + \sum_i \frac{\partial L}{\partial \dot{x}_i} d\dot{x}_i$$



Output Data

Forecasting of Space Weather

1. Physical models
2. Neural Networks
3. Local Filtering
4. NARMAX model

The main idea of PROGRESS is to combine first principles based models with Systems Science approach to achieve reliable forecast of space weather.

Participants



R. Von Fay-Siebenburgen, M. B



ILMATIETEEN LAITOS
METEOROLOGISKA INSTITUTET
FINNISH METEOROLOGICAL INSTITUTE

S. Walker, R. Boynton

N. Ganushkina, I. Sillanpaa,

S. Dubyagin



THE UNIVERSITY OF
WARWICK

T. Arber, K. Bennett



Y. Shprits



M. Liemohn, B. van der Holst



V. Yatsenko



V. Krasnoselskikh, V. Shastun



P. Wintoft, M. Wik

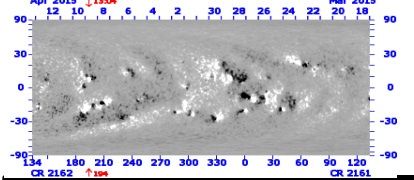
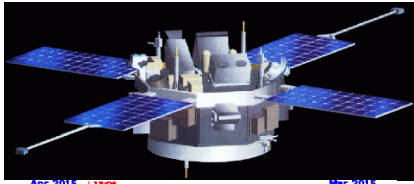
Objectives

1. Develop a European numerical MHD based model that will enable the advanced forecast of solar wind parameters at L1.
2. Use system science methodologies alongside those currently available (empirical, ANN) to forecast the evolution of geomagnetic indices in response to the solar wind.
3. Construct a new set of statistical wave models to describe the plasma wave environment of the inner magnetosphere that will accurately reflect the physics of the dynamics of the radiation belts under the influence of the solar wind.

Objectives

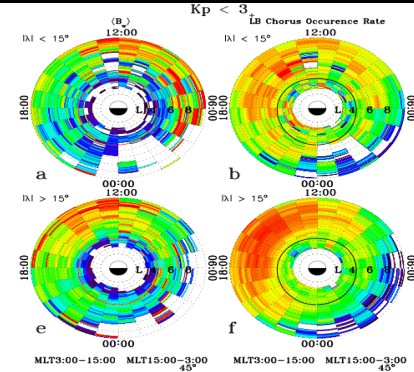
4. Incorporate forecasting capabilities into the physics based numerical model for low energy electrons IMPTAM that currently is able to provide a now-cast only.
5. Develop a novel, reliable, and accurate forecast of the radiation environment in the region of radiation belts exploiting the fusion between data based models for high energy fluxes at geostationary orbit SNB³GEO, IMPTAM, the most advanced model for high energy electrons in the radiation belts – VERB, and state of the art data assimilation methodology.
6. To combine the prediction tools for geomagnetic indices and radiation environment within the magnetosphere with the forecast of solar wind parameters at L1 and upstream of the magnetosphere to significantly increase the advance time of the forecast.

Overview



Solar wind propagation from Sun to L1 (AWSOM/SWIFT)

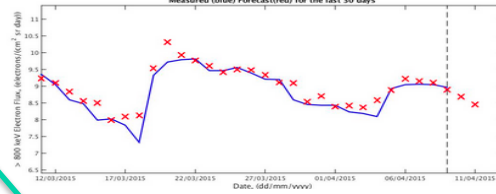
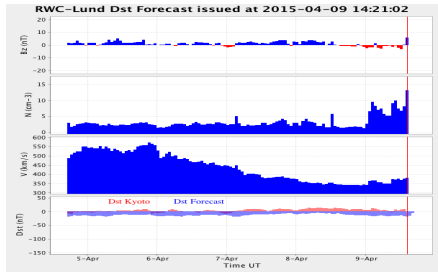
Development of new statistical models



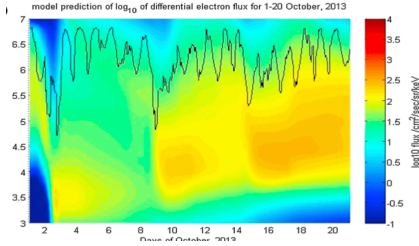
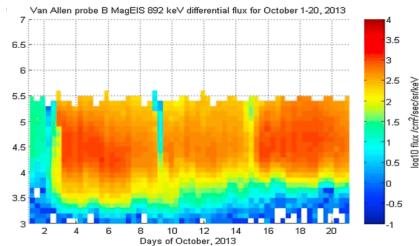
Low energy electron model

Forecast of the Evolution of Geomagnetic indices

Forecast of the high energy electron environment



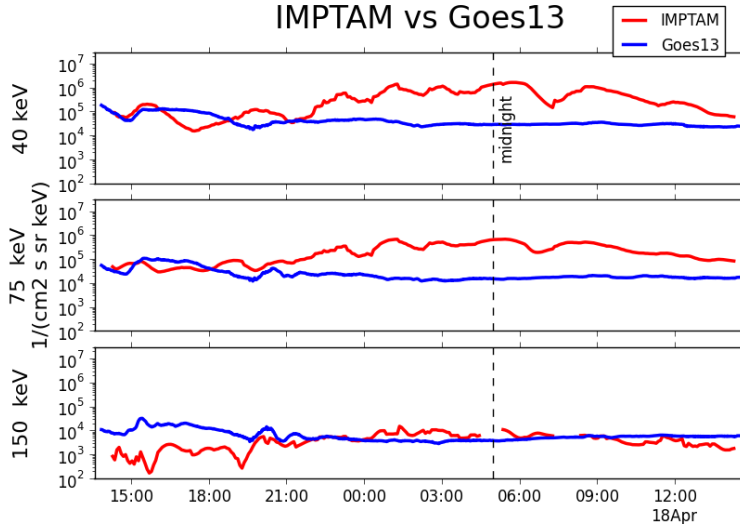
Fusion of forecast tools



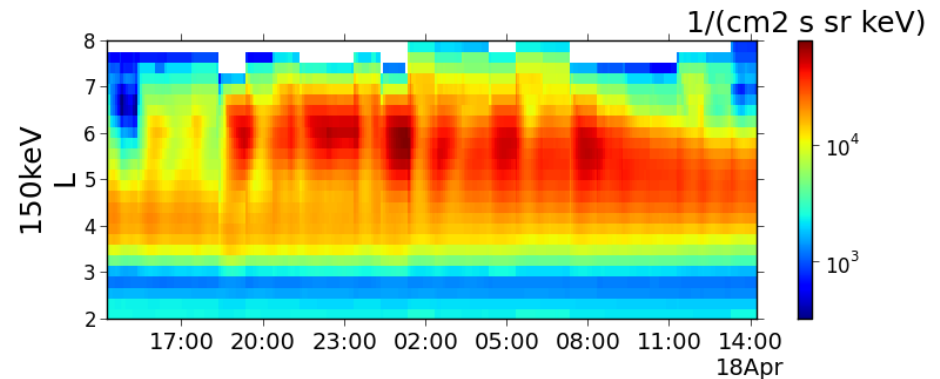
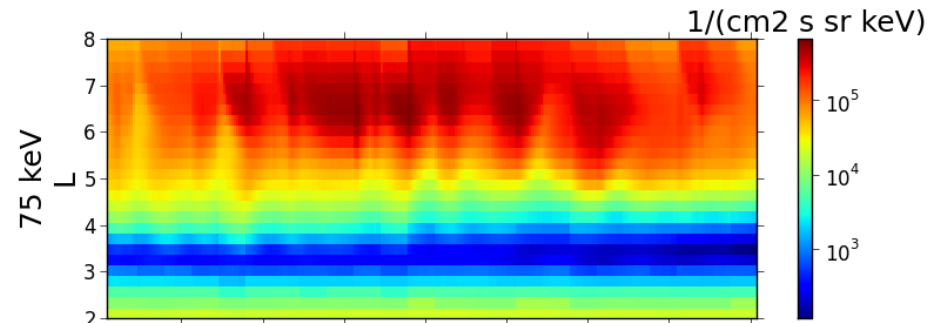
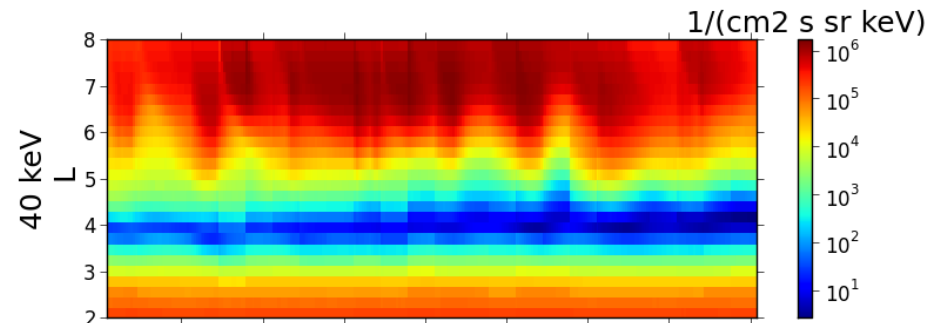
IMPTAM Low Energy Electrons

Leader -Ganushkina, FMI

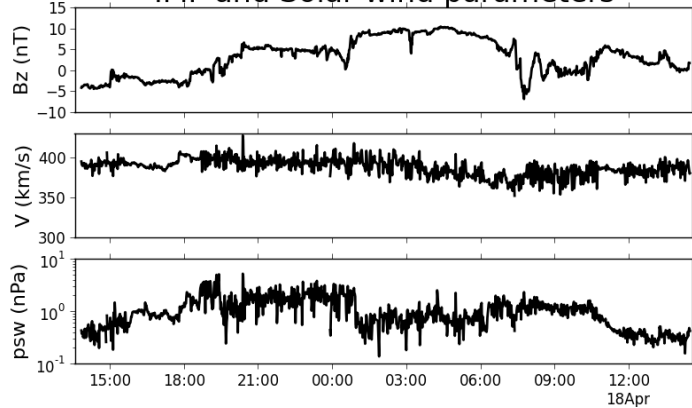
Electron fluxes at geostationary orbit
IMPTAM vs Goes13



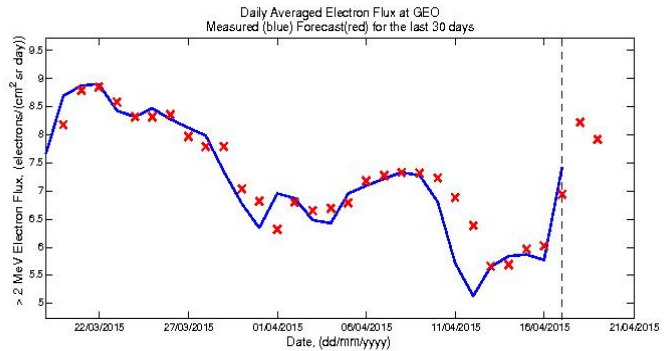
IMPTAM electron fluxes at midnight



IMF and Solar wind parameters



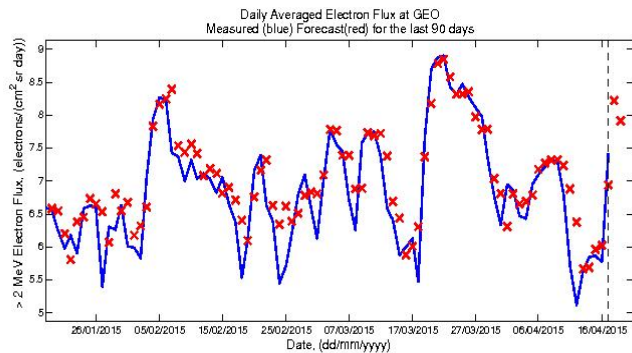
Online Forecasts – Sheffield GOES Model



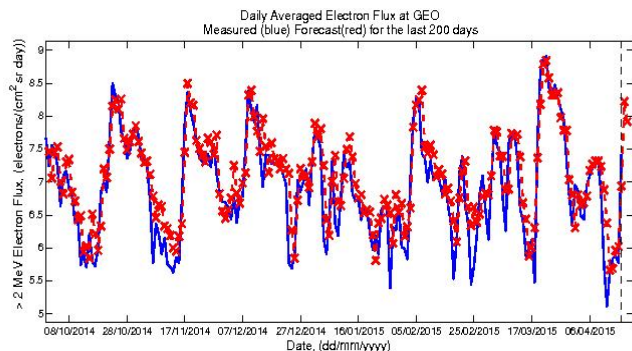
The one day ahead forecasts of the relativistic electron fluxes with energies greater than 2 MeV at GEO has been developed in Sheffield and is available in real time:

http://www.ssg.group.shef.ac.uk/USSW/2MeV_EF.html.

Past 90 days



Past 200 days



NOAA REFM Forecast

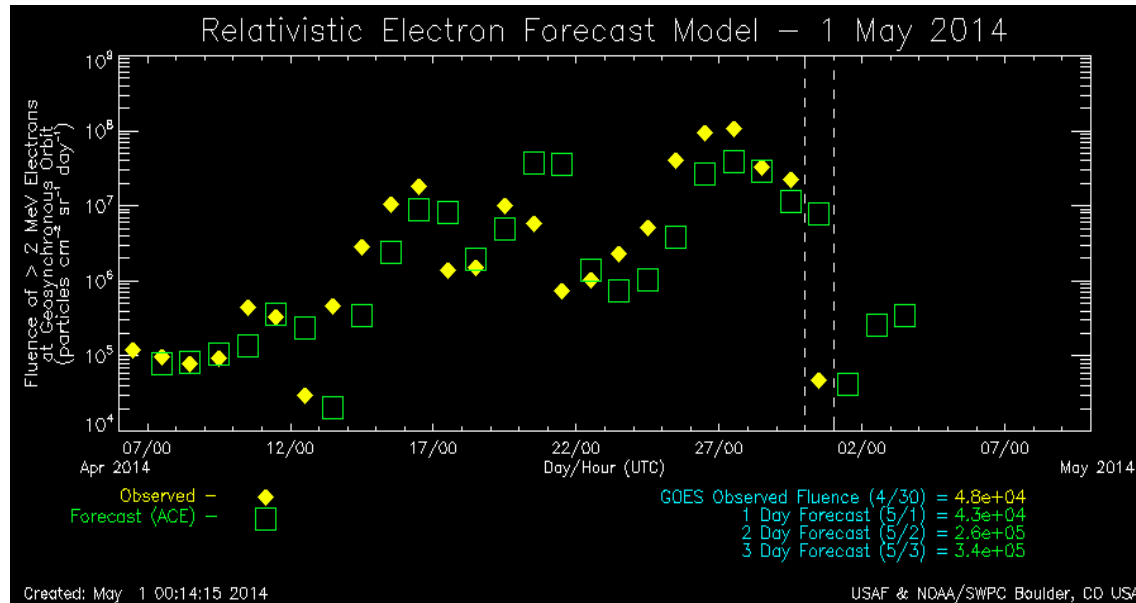
Space Weather Prediction Center

01/05/2014 21:09

NOAA / Space Weather Prediction Center

Relativistic Electron Forecast Model

Presented by the USAF and NOAA/ [Space Weather Prediction Center](#)



The impact of high-energy (relativistic) electrons on orbiting satellites can cause electric discharges across internal satellite components, which in turn leads to spacecraft upsets and/or complete satellite failures. The Relativistic Electron Forecast Model predicts the occurrence of these electrons in geosynchronous orbit. Plots and data are updated daily at 0010 UT. Dashed vertical lines indicate the last vertical value. When the input parameters are not available, the forecast is not shown.

[REFM Verification Plot](#) and [Model Documentation](#)

[1 to 3 Day Predictions](#) (text file) and corresponding [Performance Statistics](#).
Predictions created using data from the [ACE spacecraft](#).

Historical electron particle data is archived at the [National Geophysical Data Center for Solar-Terrestrial Physics](#).

Visually impaired users may [contact SWPC](#) for assistance.
Please [credit SWPC](#) when using these images.



[SWPC Home](#)

Space Weather Topics:

[Alerts / Warnings](#), [Space Weather Now](#), [Today's Space Wx](#), [Data and Products](#), [About Us](#),
[Email Products](#), [Space Wx Workshop](#), [Education/Outreach](#), [Disclaimer](#), [Customer Services](#), [Contact Us](#)

Comparison of REFM and SNB³GEO Forecasts

(01.03.2012-03.07.2014)

Balikhin, Rodriguez, Boynton, Walker, Aryan, Sibeck, Billings (submitted to SW 2015)

$$PE = 1 - \frac{1}{N} \sum \frac{(Y(t) - Ym(t))^2}{\text{var}(Y)}$$

$$C_{cor} = \frac{1}{N} \sum \frac{(Y(t) - \langle Y(t) \rangle)(Ym(t) - \langle Ym(t) \rangle)}{\sqrt{\text{var}(Ym)\text{var}(Y)}}$$

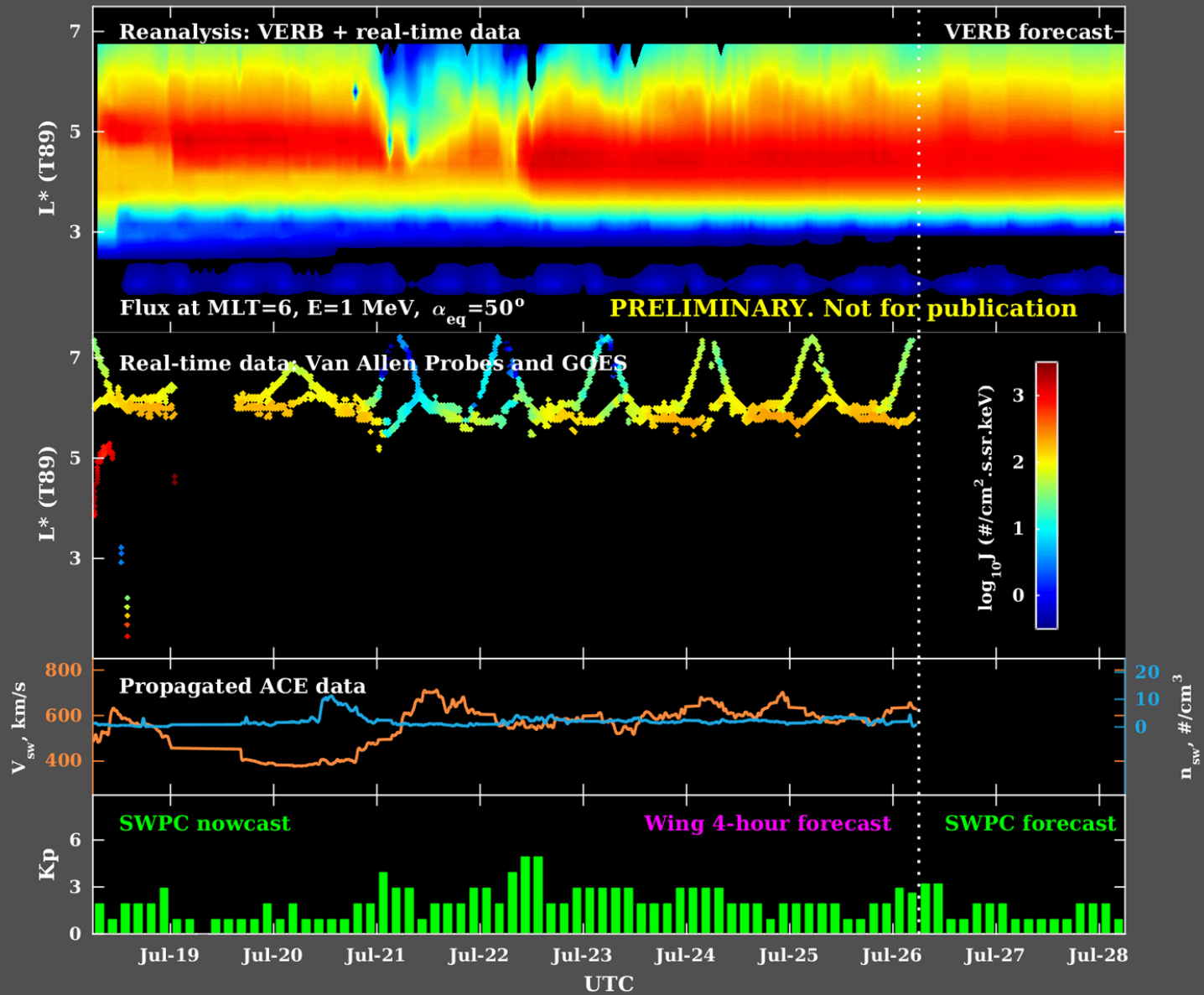
Comparison of REFM and SNB³GEO Forecasts

Balikhin, Rodriguez, Boynton, Walker, Aryan, Sibeck Billings, SW 2016

Model	Prediction Efficiency Flux	Correlation Flux	Prediction Efficiency Log Flux	Correlation Log Flux
REFM	-1.31	0.73	0.70	0.85
SNB ³ GEO	0.63	0.82	0.77	0.89

VERB (Shprits Group)

Real-time Radiation Belt Forecast, 06:00, Jul 26, 2017 UTC



PROGRESS: wave models

- Statistical Wave models and physics of wave particle interaction

A10225

MEREDITH ET AL.: GLOBAL MODEL OF WHISTLER MODE CHORUS

A10225

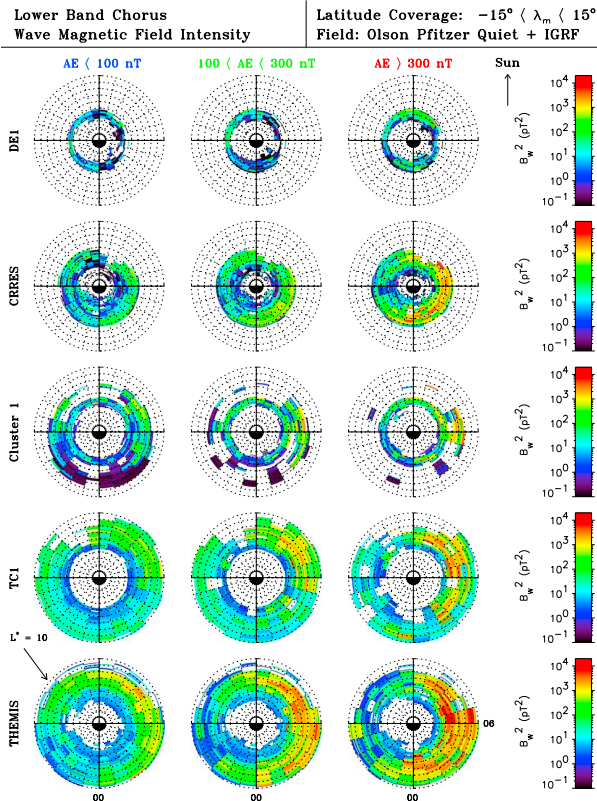
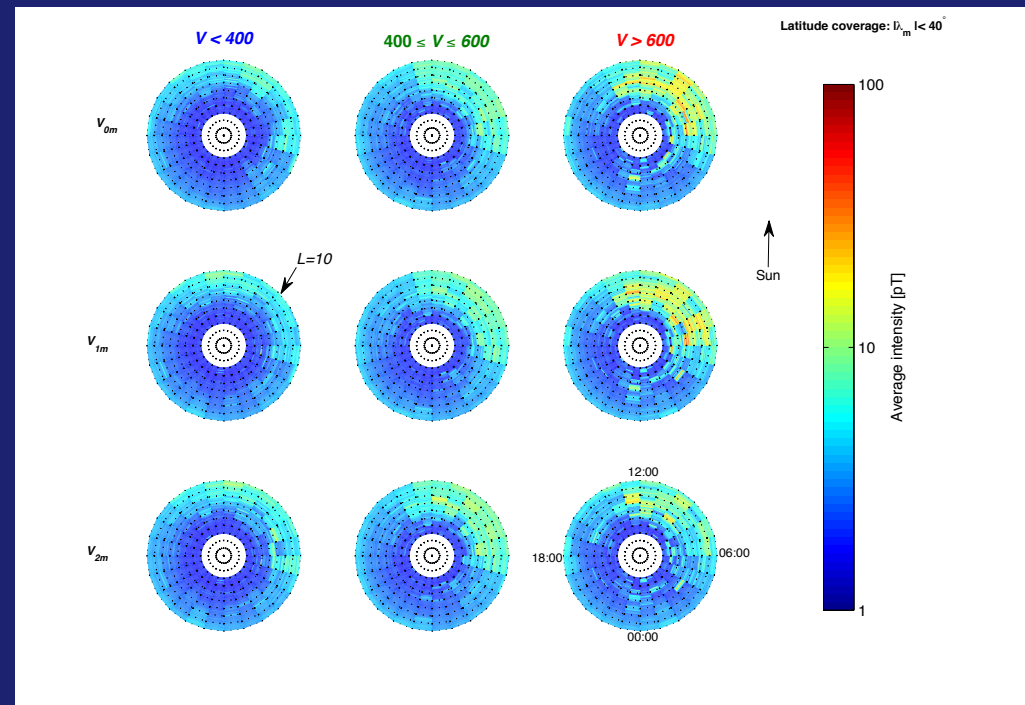


Figure 2. Equatorial wave intensity of lower band chorus as a function of L^* , MLT and geomagnetic activity for each of the five satellites.



PROGRESS

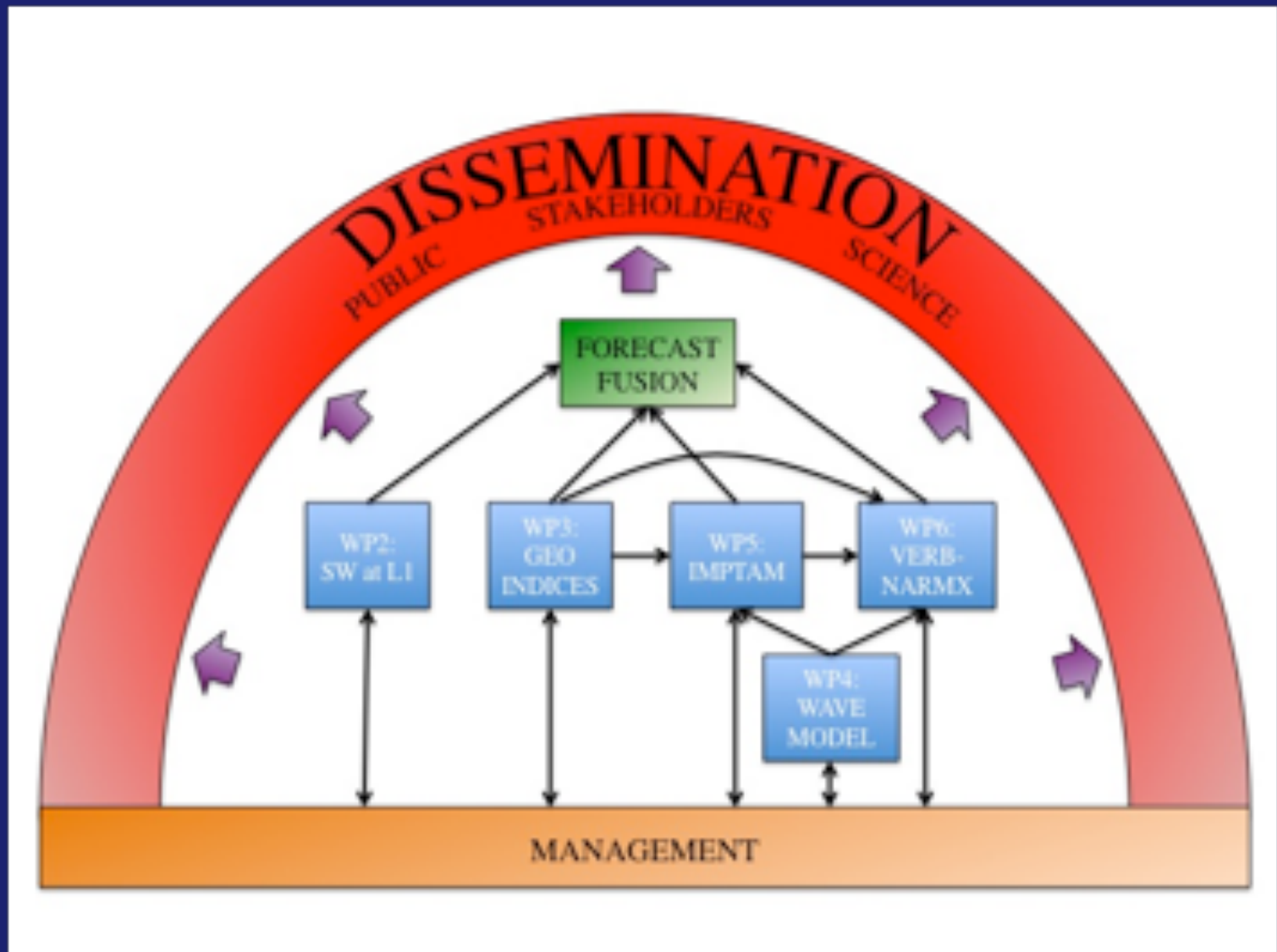


Figure 1: Workflow of project PROGRESS